

**Comparative study of Cobalt and Nickle substituted Zinc Ferrites
as Electrodes in Supercapacitors**



By

Hafiz Muhammad Ameer Hamza

(Registration No: 00000326922)

Department of Materials Engineering

School of Chemical and Materials Engineering

National University of Sciences & Technology (NUST)

Islamabad, Pakistan

(2024)

Comparative study of Cobalt and Nickle substituted Zinc Ferrites as Electrodes in Supercapacitors



By

Hafiz Muhammad Ameer Hamza

(Registration No: 00000326922)

A thesis submitted to the National University of Sciences and Technology, Islamabad,

in partial fulfillment of the requirements for the degree of

Master of Science in
Nanoscience and Engineering

Supervisor: Dr. Sofia Javed

School of Chemical and Materials Engineering

National University of Sciences & Technology (NUST)

Islamabad, Pakistan

(2024)

THESIS ACCEPTANCE CERTIFICATE



THESIS ACCEPTANCE CERTIFICATE

Certified that final copy of MS thesis written by **Mr. Hafiz Muhammad Ameer Hamza** (Registration No 00000326922), of School of Chemical & Materials Engineering (SCME) has been vetted by undersigned, found complete in all respects as per NUST Statues/Regulations, is free of plagiarism, errors, and mistakes and is accepted as partial fulfillment for award of MS degree. It is further certified that necessary amendments as pointed out by GEC members of the scholar have also been incorporated in the said thesis.

Signature: _____

Name of Supervisor: Dr. Sofia Javed

Signature (HOD): _____

Date: 20/5/21

Signature (Dean/Principal): _____

Date: 21.5.2021

TH - 1

Form TH-1



National University of Sciences & Technology (NUST)

MASTER'S THESIS WORK


Formulation of Guidance and Examination Committee (GEC)

Name: Hafiz muhammad ameer Hamza NUST Reg No: 00000326922
 Department: Department of Materials Engineering Specialization: Master of Science in Nanoscience and Engineering
 Credit Hour Completed: 24.0 CGPA: 3.38

Course Work Completed

S/No:	Code:	Title:	Core/Elective:	CH:	Grade:
1.	MSE-854	Characterization Of Materials	Compulsory	3.0	B+
2.	RM-898	Research Methodology	Additional	2.0	Q
3.	NSE-845	Nanolithography And Device Fabrication	Compulsory	3.0	C+
4.	NSE-813	Essentials of Nanoscience and Engineering	Compulsory	3.0	B+
5.	MSE-856	Nano Material and Processing	Compulsory	3.0	B+
6.	MSE-872	Composite Materials	Elective	3.0	B
7.	NSE-812	Environmental Nanotechnology	Elective	3.0	B
8.	ESE-829	Functional Nanomaterials for Renewable Energy	Elective	3.0	B
9.	NSE-845	Nanolithography And Device Fabrication	Repeat	3.0	B+
10.	NSE-961	Surface Coatings and Thin Films	Elective	3.0	A

Date 30 - May - 2022

Student's Signature 

Thesis Committee

- Name: Sofia Javed (Supervisor)
Department: Department of Materials Engineering
- Name: Muhammad Aftab Akram (Cosupervisor)
Department: Department of Materials Engineering
- Name: Mohsin Saleem (Internal)
Department: Department of Materials Engineering
- Name: Zeeshan Ali (Internal)
Department: Department of Materials Engineering
- Name: Iftikhar Hussain Gul (Internal)
Department: Department of Materials Engineering

Signature 
 Signature 
 Signature 
 Signature 
 Signature 

Date: 30 - May - 2022

Signature of Head of Department: 

APPROVAL

Date: 30 - May - 2022

Signature of Dean/Principal: 

TH - 4



National University of Sciences & Technology (NUST)

FORM TH-4

MASTER'S THESIS WORK

We hereby recommend that the dissertation prepared under our supervision by
Regn No & Name: 00000326922 Hafiz Muhammad Ameer Hamza

Title: Comparative Study of Cobalt and Nickel Substituted Zinc Ferrites as Electrodes in Supercapacitors.

Presented on: 04 Apr 2024 at: 1200 hrs in SCME Seminar Hall

Be accepted in partial fulfillment of the requirements for the award of Masters of Science degree in Nano Science & Engineering.

Guidance & Examination Committee Members

Name: Dr Zeeshan Ali

Signature: [Signature]

Name: Dr Mohsin Saleem

Signature: [Signature]

Name: Dr Iftikhar Hussain Gul

Signature: [Signature]

Name: Dr Muhammad Aftab Akram (Co-Supervisor)

Signature: [Signature]

Supervisor's Name: Dr Sofia Javed

Signature: [Signature]

Dated: 26.4.24

[Signature]

Head of Department

Date 28/4/24

[Signature]

Dean/Principal

Date 28.4.2024

AUTHOR'S DECLARATION

I Hafiz Muhammad Ameer Hamza hereby state that my MS thesis titled “Comparative study of Cobalt and Nickle substituted Zinc Ferrites as Electrodes in Supercapacitors” is my own work and has not been submitted previously by me for taking any degree from National University of Sciences and Technology, Islamabad or anywhere else in the country/ world.

At any time if my statement is found to be incorrect even after I graduate, the university has the right to withdraw my MS degree.

Name of Student: Hafiz Muhammad Ameer Hamza

Date: 16 May 2024

PLAGIARISM UNDERTAKING

I solemnly declare that research work presented in the thesis titled “Comparative study of Cobalt and Nickle substituted Zinc Ferrites as Electrodes in Supercapacitors” is solely my research work with no significant contribution from any other person. Small contribution/help wherever taken has been duly acknowledged and that complete thesis has been written by me.

I understand the zero-tolerance policy of the HEC and National University of Sciences and Technology (NUST), Islamabad towards plagiarism. Therefore, I as an author of the above titled thesis declare that no portion of my thesis has been plagiarized and any material used as reference is properly referred/cited.

I undertake that if I am found guilty of any formal plagiarism in the above titled thesis even after award of MS degree, the University reserves the rights to withdraw/revoke my MS degree and that HEC and NUST, Islamabad has the right to publish my name on the HEC/University website on which names of students are placed who submitted plagiarized thesis.

Student Signature: 

Name: Hafiz Muhammad Ameer Hamza

DEDICATION

“I dedicate this thesis to my beloved family and cherished friends, whose unwavering support, encouragement, and belief in my abilities have been the driving force behind my academic journey.”

ACKNOWLEDGEMENTS

I would like to express my deepest gratitude to my supervisor, Dr. Sofia Javed, for her invaluable guidance, unwavering support, and insightful feedback throughout the course of this thesis. Her expertise and encouragement have been instrumental in shaping the direction of my research.

I extend my heartfelt thanks to the faculty members of the SCME for their constructive critiques and valuable input, which have greatly enriched the quality of this work.

I am grateful to my colleagues and friends who provided assistance and encouragement during challenging times. Their camaraderie has made this academic journey more enjoyable and rewarding.

Special thanks to my family for their unending love, encouragement, and understanding. Their constant support has been my pillar of strength.

This thesis is a culmination of the collective efforts and support from all those who have been a part of my academic and personal journey. Thank you for being an integral part of this endeavor.

Hafiz Muhammad Ameer Hamza

TABLE OF CONTENTS

ACKNOWLEDGEMENTS	IX
TABLE OF CONTENTS	X
LIST OF TABLES	XII
LIST OF FIGURES	XIII
LIST OF SYMBOLS, ABBREVIATIONS AND ACRONYMS	XIV
ABSTRACT	XV
CHAPTER 1: INTRODUCTION	1
1.1 Concept of Nanotechnology	1
1.2 Introduction to Ferrites	1
1.3 Background History of Ferrites	1
1.4 Classification of Ferrites	2
1.4.1 Soft Ferrites	2
1.4.2 Hard Ferrites	2
1.5 Types of Ferrites	3
1.5.1 Cubic Ferrites	3
1.5.2 Hexagonal Ferrites	4
1.5.3 Advantages of Ferrites	5
1.5.4 Application of Ferrites	6
1.6 Objectives of the Research	7
CHAPTER 2: LITERATURE REVIEW	8
2.1 Introduction to Supercapacitors and Their Importance	8
2.2 Electrode Materials in Supercapacitors	8
2.3 Zinc Ferrites as Electrode Materials	9
2.4 Cobalt-Substituted Zinc Ferrites	10
2.5 Nickel-Substituted Zinc Ferrites	10
2.6 Factors Affecting Supercapacitor Performance	11
2.7 Recent Advances in Synthesis and Characterization	11
2.8 Comparative Studies	12
2.9 Challenges and Future Directions	13
2.10 Research Gap and Rationale	14
CHAPTER 3: MATERIALS AND METHODS	15
3.1 Techniques for Synthesis of Nanomaterials	15
3.2 Top-Down Approaches	15
3.2.1 Mechanical Milling	16
3.2.2 Laser Ablation	16
3.3 Bottom-Up Approaches	17
3.3.1 Sol-Gel Method	17
3.3.2 Micro Emulsion	18

3.3.3	Solvothermal or Hydrothermal	19
3.3.4	Chemical Co-Precipitation	19
3.4	Synthesis of ZnFe₂O₄ Magnetic Nanoparticles	20
3.5	Synthesis of Zn_{0.5}Ni_{0.5}Fe₂O₄ and Zn_{0.5}Co_{0.5}Fe₂O₄ Nanoparticles	21
CHAPTER 4: CHARACTERIZATION		23
4.1	X-Ray Diffraction techniques	23
4.1.1	Principle:	23
4.1.2	Relevance to Research:	23
4.2	Scanning Electron Microscopy (SEM)	24
4.2.1	Principle:	24
4.2.2	Relevance to Research:	24
4.3	Fourier Transform Infrared Spectroscopy (FTIR)	25
4.3.1	Principle:	25
4.3.2	Relevance to Research:	25
4.4	Raman Spectroscopy	26
4.4.1	Principle:	26
4.4.2	Relevance to Research:	26
4.5	Dielectric Analysis	27
4.5.1	Principle:	27
4.5.2	Relevance to Research:	27
4.6	Cyclic Voltammetry	28
4.6.1	Principle:	28
4.6.2	Relevance to Research:	29
CHAPTER 5: RESULTS AND DISCUSSION		30
5.1	X-Ray Diffraction Spectroscopy	30
5.2	Scanning Electron Microscopy	32
5.3	Raman Spectroscopy	33
5.4	Fourier-Transform Infrared Spectroscopy	35
5.5	Dielectric	38
5.5.1	Imaginary part of Dielectric Permittivity	39
5.5.2	Dielectric Loss	39
5.5.3	Real part of Impedance	40
5.5.4	Imaginary part of Impedance	41
5.5.5	AC Conductivity	41
5.6	Electrochemical Testing	42
CHAPTER 6: CONCLUSIONS AND FUTURE RECOMMENDATION		45
6.1	Conclusion	45
6.2	Future Recommendations	46
REFERENCES		47

LIST OF TABLES

Table 5.1: Properties of ZnFe_2O_4 , $\text{Zn}_{0.5}\text{Ni}_{0.5}\text{Fe}_2\text{O}_4$ and $\text{Zn}_{0.5}\text{Co}_{0.5}\text{Fe}_2\text{O}_4$ Nanoparticles	31
--	----

LIST OF FIGURES

Figure 1.1: Crystal Structure of Spinel Ferrite	3
Figure 1.2: Crystal Structure of Garnet Ferrite	4
Figure 1.3: Crystal Structure of Hexagonal Ferrite	5
Figure 3.1: Top down and bottom-up approaches.....	15
Figure 3.2: Principle of mechanical milling	16
Figure 3.3: Working principle of Laser Ablation	17
Figure 3.4: Steps involved in Sol Gel Method	18
Figure 3.5: Microemulsion technique for nanoparticle synthesis.....	18
Figure 3.6: Hydrothermal synthesis of Nanoparticles	19
Figure 3.7: Coprecipitation Method Synthesis Nanoparticles.....	20
Figure 3.8: Schematic diagram of the synthesis of $ZnFe_2O_4$, $Zn_{0.5}Ni_{0.5}Fe_2O_4$ and $Zn_{0.5}Co_{0.5}Fe_2O_4$	22
Figure 4.1: Working principle of XRD	23
Figure 4.2: Working principle of Scanning Electron Microscope.....	24
Figure 4.3: Working principle of FTIR.....	25
Figure 4.4: Working principle of Raman Spectroscopy.....	26
Figure 4.5: Working principle of Dielectric	27
Figure 4.6: Working principle of cyclic voltammetry	28
Figure 5.1: The X-Ray diffraction Pattern of $ZnFe_2O_4$, $Zn_{0.5}Ni_{0.5}Fe_2O_4$ and $Zn_{0.5}Co_{0.5}Fe_2O_4$ Nanoparticles.....	31
Figure 5.2: SEM images of $ZnFe_2O_4$, $Zn_{0.5}Ni_{0.5}Fe_2O_4$ and $Zn_{0.5}Co_{0.5}Fe_2O_4$ Nanoparticles	32
Figure 5.3: EDS spectrum of $ZnFe_2O_4$, $Zn_{0.5}Ni_{0.5}Fe_2O_4$ and $Zn_{0.5}Co_{0.5}Fe_2O_4$ Nanoparticles	32
Figure 5.4: Raman Shift of $ZnFe_2O_4$, $ZnNiFe_2O_4$ and $ZnCoFe_2O_4$ Nanoparticles	34
Figure 5.5: The X-Ray diffraction Pattern of $ZnFe_2O_4$, $Zn_{0.5}Ni_{0.5}Fe_2O_4$ and $Zn_{0.5}Co_{0.5}Fe_2O_4$ Nanoparticles	36
Figure 5.6: Dielectric properties of $ZnFe_2O_4$, $Zn_{0.5}Ni_{0.5}Fe_2O_4$ and $Zn_{0.5}Co_{0.5}Fe_2O_4$ Nanoparticles	38
Figure 5.7: Cyclic Voltammetry properties of $ZnFe_2O_4$, $Zn_{0.5}Ni_{0.5}Fe_2O_4$ and $Zn_{0.5}Co_{0.5}Fe_2O_4$ Nanoparticles.....	42

LIST OF SYMBOLS, ABBREVIATIONS AND ACRONYMS

EDX	Energy Dispersive X-Ray
SEM	Scanning Electron Microscope
XRD	X-ray Powder Diffraction
FTIR	Fourier-Transform Infrared Spectroscopy
nm	Nanometers
MNPs	Magnetic Nanoparticles
CV	Cyclic Voltammetry

ABSTRACT

The potential of Zinc Ferrite (ZnFe_2O_4) and its derivatives, namely zinc-nickel ferrite ($\text{Zn}_{0.5}\text{Ni}_{0.5}\text{Fe}_2\text{O}_4$) and zinc cobalt ferrite ($\text{Zn}_{0.5}\text{Co}_{0.5}\text{Fe}_2\text{O}_4$), as promising materials for supercapacitor electrodes is explored in this study. Significant attention has been garnered by these materials due to their exceptional combination of high electrical conductivity and chemical stability, essential attributes for efficient energy storage devices. To investigate their suitability, nanoparticles of ZnFe_2O_4 , $\text{Zn}_{0.5}\text{Ni}_{0.5}\text{Fe}_2\text{O}_4$, and $\text{Zn}_{0.5}\text{Co}_{0.5}\text{Fe}_2\text{O}_4$ were synthesized using the co-precipitation technique. A thorough characterization of these nanoparticles was then conducted using various analytical methods, including X-ray Diffraction, Scanning Electron Microscopy, Energy-Dispersive X-ray Spectroscopy, Fourier Transform Infrared Spectroscopy, and Raman Spectroscopy. Valuable insights into the structural and chemical properties of nanoparticles were provided by these analyses. Furthermore, the electrochemical behavior of these nanoparticles was examined through Cyclic Voltammetry, Galvanostatic Charge-Discharge analysis, and Dielectric Spectroscopy. Promising results were revealed by these electrochemical studies, confirming the presence of a spinel crystal structure within the nanoparticles, indicative of their excellent electrochemical performance. In light of our combined findings, the potential applicability of ZnFe_2O_4 , $\text{Zn}_{0.5}\text{Ni}_{0.5}\text{Fe}_2\text{O}_4$, and $\text{Zn}_{0.5}\text{Co}_{0.5}\text{Fe}_2\text{O}_4$ nanoparticles as promising supercapacitor electrodes is strongly supported by this study. The presence of a spinel crystal structure within the nanoparticles, indicative of their excellent electrochemical performance, was confirmed by these electrochemical studies. These results contribute significantly to the growing body of knowledge on advanced electrode materials for energy storage applications. Moreover, the groundwork for further in-depth exploration and optimization of these unique ferrite-based nanoparticulate systems is laid by this research, offering promising prospects for the development of high-performance supercapacitors in the future.

Keywords: Ferrites, Electrochemical Properties, Supercapacitor.

CHAPTER 1: INTRODUCTION

1.1 Concept of Nanotechnology

Nanotechnology represents a groundbreaking scientific and technological paradigm that has dramatically transformed the landscape of material science and engineering. At the core of nanotechnology is the manipulation of matter at the nanoscale, typically in the range of 1 to 100 nanometers. This allows for the deliberate design and fabrication of materials with unprecedented precision and control over their properties. The ability to engineer materials at such a small scale has opened up a multitude of possibilities in various fields, including electronics, energy storage, medicine, and more[1].

Nanotechnology enables the creation of novel materials with unique properties and functionalities. These materials often exhibit quantum effects, enhanced surface area, and superior mechanical, electrical, and thermal properties compared to their bulk counterparts. In the context of energy storage, nanomaterials play a pivotal role in the development of high-performance supercapacitors, which are essential for addressing the ever-growing demand for efficient and sustainable energy storage solutions[2].

1.2 Introduction to Ferrites

Ferrites, as a class of ceramic materials, have garnered significant attention due to their exceptional magnetic and electrical properties. These materials are composed of iron (Fe) cations and oxygen (O) anions, typically represented as MFe_2O_4 , where M denotes a divalent metal cation. The unique arrangement of ions in the crystal lattice of ferrites results in their distinctive magnetic and electrical behavior. Ferrites are versatile materials that have found applications in diverse fields, including telecommunications, electronics, medicine, and more[3].

1.3 Background History of Ferrites

The historical development of ferrites can be traced back to the early 20th century when scientists began exploring their magnetic properties. In 1930, Kato and Takei

successfully synthesized the first ferrite, which they initially referred to as spinel ferrite. This milestone marked the beginning of extensive research into the properties and applications of ferrites. Over the decades, ferrites have evolved from being mere scientific curiosities to becoming integral components in a wide range of technological devices and systems[4].

The historical journey of ferrites is closely intertwined with the evolution of technology itself. From their early use in radio antennas and magnetic cores for transformers to their modern applications in data storage and medical imaging, ferrites have continually proven their versatility and adaptability[5].

1.4 Classification of Ferrites

Ferrites can be broadly classified into two main categories based on their magnetic behavior:

1.4.1 Soft Ferrites

Soft ferrites are characterized by their low coercivity, which means they exhibit low resistance to changes in magnetization. This property makes them highly responsive to external magnetic fields. As a result, soft ferrites are primarily employed in electromagnetic devices where rapid and reversible changes in magnetization are desirable. Key applications include the cores of transformers, inductors, and magnetic shielding materials[6].

1.4.2 Hard Ferrites

Conversely, hard ferrites possess high coercivity, which means they can maintain their magnetization even in the absence of an external magnetic field. This property is crucial for creating permanent magnets and magnetic storage devices such as hard disk drives and magnetic tapes[6].

1.5 Types of Ferrites

Ferrites encompass a wide range of materials, each with its own crystal structure and properties. Understanding these various types is essential for harnessing the unique characteristics of ferrites for specific applications:

1.5.1 Cubic Ferrites

Cubic ferrites, commonly referred to as spinel ferrites, are characterized by their face-centered cubic (FCC) crystal structure. This structure consists of metal cations occupying both tetrahedral and octahedral sites within the lattice. The distinctive arrangement of cations and anions in spinel ferrites gives rise to their remarkable magnetic and electrical properties[7].

1.5.1.1 Crystal Structure and Properties of Spinel Ferrites

The FCC crystal structure of spinel ferrites leads to several notable properties, including high magnetic permeability and low eddy current losses. These properties make spinel ferrites ideal for high-frequency applications such as transformers, antennas, and microwave devices. The cubic symmetry of the lattice also results in isotropic properties, which can be advantageous in certain applications[8].

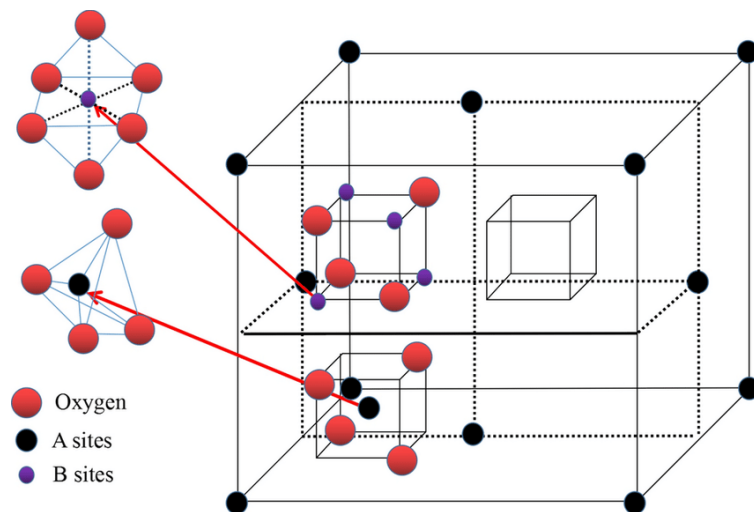


Figure 1.1: Crystal Structure of Spinel Ferrite

1.5.1.2 Garnet Ferrites

Garnet ferrites represent a subclass of cubic ferrites with a more complex crystal structure. They are known for their excellent optical properties, making them valuable in magneto-optical applications. Additionally, garnet ferrites possess unique magnetic characteristics, making them suitable for use in optical isolators, magneto-optical sensors, and optical communication systems[8].

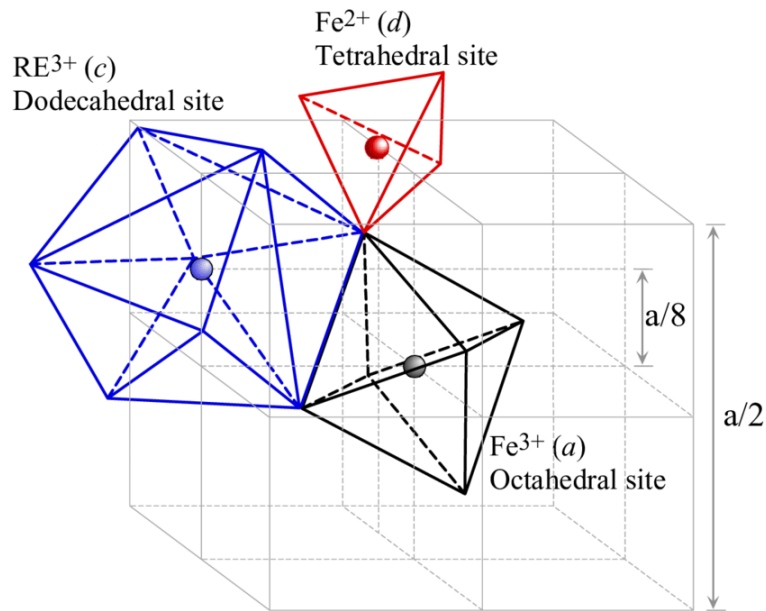


Figure 1.2: Crystal Structure of Garnet Ferrite

1.5.2 Hexagonal Ferrites

Hexagonal ferrites, often referred to as hexaferrites, feature a hexagonal crystal structure. This structural arrangement results in anisotropic magnetic properties, meaning the magnetic behavior of hexaferrites varies with direction. This property is advantageous in applications requiring directional magnetization control[8].

Hexaferrites find widespread use in microwave devices, data storage, and magnetic sensors, where their anisotropic magnetic properties can be tailored to specific needs. These applications leverage the ability of hexaferrites to exhibit high magnetic coercivity along certain crystallographic directions[9].

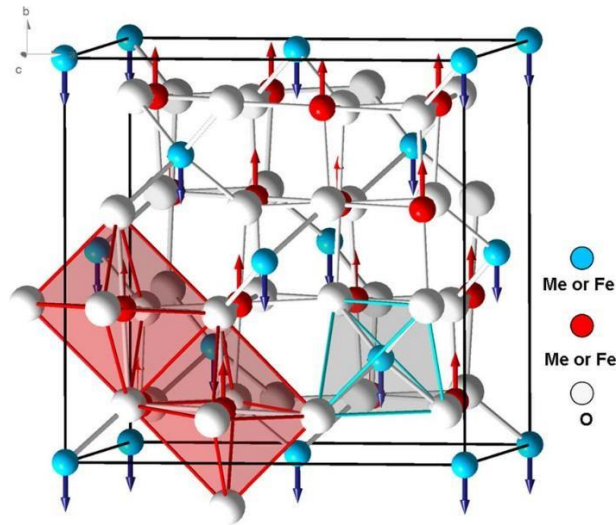


Figure 1.3: Crystal Structure of Hexagonal Ferrite

1.5.3 Advantages of Ferrites

Ferrites offer a range of advantages that make them indispensable in various applications:

High Resistivity: Ferrites exhibit high electrical resistivity, reducing eddy current losses in magnetic devices and enabling efficient operation at high frequencies.

Low Eddy Current Losses: The low conductivity of ferrites results in minimal energy loss due to eddy currents, making them ideal for high-frequency applications.

Thermal Stability: Ferrites maintain their magnetic properties over a wide temperature range, ensuring reliable performance in diverse environments.

Versatility: The ability to tailor the properties of ferrites through chemical composition and crystal structure modification allows for customization to suit specific application requirements[10].

1.5.4 Application of Ferrites

The versatility and unique properties of ferrites have led to their adoption in a wide array of applications. These applications highlight the importance of ferrites in various technological fields:

Magnetic Recording: Ferrites serve as crucial components in hard disk drives and magnetic tapes, where they enable the storage and retrieval of digital data.

Electromagnetic Interference (EMI) Suppression: Ferrite cores are widely employed to mitigate electromagnetic interference in electronic circuits and cables. Their ability to absorb and suppress unwanted electromagnetic radiation is essential for ensuring the proper functioning of electronic devices[11].

Medical Imaging: Magnetic nanoparticles based on ferrites play a pivotal role in magnetic resonance imaging (MRI). These nanoparticles provide contrast enhancement, allowing for the visualization of tissues and structures within the human body with high precision[12].

Microwave Devices: Ferrites are indispensable in the design of microwave circulators and isolators. These devices utilize the unique anisotropic properties of ferrites to control the direction of electromagnetic waves, enabling efficient signal transmission and isolation.

Antennas and Radars: Ferrite materials find application in the cores of antennas and radar absorbers. Their magnetic properties enhance the performance of these devices, enabling signal reception and transmission over a wide frequency range.[9]

Magnetic Sensors: Ferrite-based magnetic sensors are employed in a myriad of applications, including compasses, position sensors, and automotive applications. These sensors detect changes in magnetic fields and convert them into electrical signals, providing critical data for navigation and control systems[12].

1.6 Objectives of the Research

The primary objective of this research is to conduct a comprehensive comparative study of nickel (Ni) and cobalt (Co) substituted zinc ferrite (ZnFe_2O_4) for their potential application in supercapacitors. This study aims to investigate and compare the electrochemical properties, capacitive behavior, and overall performance of Ni-substituted and Co-substituted zinc ferrite-based supercapacitors. The research will encompass a multifaceted approach, including the synthesis, characterization, and evaluation of these materials, with the goal of advancing the field of energy storage through the exploration of novel ferrite-based supercapacitors.

By gaining a deeper understanding of the electrochemical behavior and energy storage capabilities of Ni and Co substituted ZnFe_2O_4 ferrites, this research seeks to contribute valuable insights to the field of energy storage technology. Subsequent chapters will delve into the methodology, experimental procedures, and results, providing a comprehensive analysis of the research findings and their implications for the future of energy storage systems.

CHAPTER 2: LITERATURE REVIEW

2.1 Introduction to Supercapacitors and Their Importance

Supercapacitors, also known as electrochemical capacitors or ultracapacitors, are energy storage devices with a unique ability to store and deliver energy rapidly. Unlike traditional batteries, supercapacitors store energy electrostatically, allowing for rapid charging and discharging cycles. They are characterized by high power density, which makes them particularly suitable for applications that require quick bursts of energy, such as regenerative braking in electric vehicles (EVs) and smoothing out fluctuations in renewable energy sources like wind and solar. Supercapacitors play a vital role in enhancing the efficiency and reliability of various systems, and their importance continues to grow as technology advances[13].

The applications of supercapacitors span a wide range of industries, from consumer electronics to transportation and renewable energy. In consumer electronics, supercapacitors are used for backup power, extending battery life, and providing rapid energy boosts. In EVs, they can capture and store energy during regenerative braking, improving overall energy efficiency. Additionally, supercapacitors are employed in renewable energy systems to store excess energy for later use, helping to stabilize power grids. As the demand for energy storage solutions increases, the development and optimization of supercapacitors and their constituent materials become a crucial area of research[14].

2.2 Electrode Materials in Supercapacitors

Electrode materials are fundamental components of supercapacitors and significantly influence their performance. These materials are responsible for storing energy through the adsorption of ions at the electrode-electrolyte interface. The ideal electrode material possesses a high surface area to maximize ion adsorption, excellent electrical conductivity for efficient charge transfer, and stability over a large number of charge/discharge cycles. Commonly used electrode materials include activated carbon, carbon nanotubes, and metal oxides. The choice of electrode material depends on the

specific application and desired performance characteristics, highlighting the importance of research in this area[15].

The role of electrode materials in supercapacitors extends beyond energy storage capacity. They also impact other crucial parameters such as specific capacitance (the ability to store charge), cycling stability (the ability to maintain performance over many charge/discharge cycles), and impedance (the resistance to charge transfer). Optimizing electrode materials is essential to enhance supercapacitor performance and expand their applications. This literature review focuses on zinc ferrites as a potential electrode material and compares their electrochemical behavior to traditional electrode materials like activated carbon, with a specific emphasis on the impact of cobalt and nickel substitution[16].

2.3 Zinc Ferrites as Electrode Materials

Zinc ferrites, a class of magnetic materials with the chemical formula $ZnFe_2O_4$, have garnered interest in recent years due to their potential as electrode materials in supercapacitors. These materials possess intriguing properties, including high electrical conductivity and chemical stability. Moreover, their magnetic properties can be tailored for various applications, making them versatile candidates for energy storage systems. Previous research has explored their use in supercapacitors and has indicated that zinc ferrites can offer competitive specific capacitance values, making them suitable for energy storage applications[17].

Some key studies have demonstrated the promising electrochemical performance of zinc ferrite-based supercapacitors. However, there remains a need for further investigation into their cycling stability and rate capability, as these are critical factors in assessing their practicality as electrode materials. The present study aims to address this gap by conducting a comparative analysis of zinc ferrites with cobalt and nickel substitution to determine their suitability for supercapacitor applications. The insights gained will contribute to a deeper understanding of zinc ferrites as electrode materials and their potential advantages and challenges in energy storage systems[18, 19].

2.4 Cobalt-Substituted Zinc Ferrites

Cobalt-substituted zinc ferrites (CZF) have gained attention as potential electrode materials in supercapacitors. The introduction of cobalt into the crystal structure of zinc ferrites can alter their electrochemical properties. Studies by Zhu et al. (2018) have shown that CZF can exhibit enhanced specific capacitance and improved cycling stability compared to pure zinc ferrites. This enhancement can be attributed to the synergistic effects of cobalt substitution, which modifies the electronic structure and enhances the overall electrochemical performance. However, it's essential to note that the specific cobalt substitution ratio, synthesis method, and characterization techniques can significantly influence the material's performance[20, 21].

To date, limited research has comprehensively compared CZF with other electrode materials commonly used in supercapacitors, such as activated carbon or carbon nanotubes. This comparative aspect is vital for understanding the advantages and potential limitations of CZF. By conducting a thorough comparative analysis of CZF with other materials, this study aims to shed light on the suitability of CZF for specific supercapacitor applications and contribute to the broader understanding of cobalt-substituted materials in energy storage.

2.5 Nickel-Substituted Zinc Ferrites

Nickel-substituted zinc ferrites (NZF) have also emerged as a subject of interest in the realm of supercapacitor electrode materials. Nickel's incorporation into the crystal lattice of zinc ferrites can lead to improved electrical conductivity and favorable electrochemical properties. Research by Bhavsar et al. (2020) has demonstrated the potential of NZF in supercapacitors, showcasing high specific capacitance and excellent cycling stability. However, it's worth noting that the specific nickel substitution ratio plays a critical role in determining the material's electrochemical behavior[22, 23].

To advance the field and make informed choices regarding electrode materials, it is crucial to conduct a direct comparison between NZF and other commonly used electrode materials. This comparison includes evaluating NZF against cobalt-substituted zinc ferrites

to understand how the choice of substitution affects supercapacitor performance. The forthcoming comparative study aims to elucidate the strengths and weaknesses of NZF in practical applications, providing valuable insights for researchers and engineers seeking optimal electrode materials for supercapacitors[8].

2.6 Factors Affecting Supercapacitor Performance

Supercapacitor performance is influenced by several key factors, including specific capacitance, cycling stability, and impedance. Specific capacitance measures the charge storage capacity of the electrode material and is a critical parameter for determining energy density. Cycling stability assesses the material's ability to maintain its performance over a large number of charge/discharge cycles, which is crucial for long-term device reliability. Impedance reflects the ease with which charge can transfer between the electrode and electrolyte, impacting the rate capability of supercapacitors. The choice of electrode material plays a pivotal role in determining these performance parameters[24, 25].

Cobalt and nickel substitution in zinc ferrites can modify these factors due to changes in the material's electronic structure and conductivity. While previous research has examined the electrochemical behavior of cobalt and nickel-substituted zinc ferrites, a comprehensive comparison between these materials is lacking. This literature review underscores the importance of understanding how cobalt and nickel substitution impacts these key performance factors and highlights the need for a systematic comparative study[26].

2.7 Recent Advances in Synthesis and Characterization

Recent advances in the synthesis and characterization of electrode materials have significantly contributed to the development of supercapacitors. Traditional synthesis methods, such as sol-gel and hydrothermal processes, have been refined and optimized to tailor the properties of electrode materials. For instance, Yadav et al. (2021) have demonstrated the successful synthesis of cobalt and nickel-substituted zinc ferrites with controlled composition and morphology, allowing for precise tuning of electrochemical performance[27].

In addition to advanced synthesis techniques, modern characterization tools have played a pivotal role in elucidating the structural and electrochemical properties of these materials. X-ray diffraction (XRD), scanning electron microscopy (SEM), and electrochemical impedance spectroscopy (EIS) are among the tools commonly used to analyze the physical and electrochemical characteristics of electrode materials. These techniques enable researchers to gain insights into the crystal structure, surface morphology, and charge transfer processes, providing essential information for optimizing material performance[28].

The integration of advanced synthesis methods and state-of-the-art characterization techniques offers researchers valuable tools to design and analyze cobalt and nickel-substituted zinc ferrites for supercapacitor applications. These innovations are instrumental in advancing the field and are pertinent to the forthcoming comparative study's methodology.

2.8 Comparative Studies

Comprehensive comparative analyses between cobalt and nickel-substituted zinc ferrites (CZF and NZF) and other commonly used electrode materials in supercapacitors are limited. Most existing studies focus on a single material, lacking direct comparisons that can inform material selection for specific applications. This section emphasizes the necessity of systematic comparative studies that provide a holistic understanding of material performance[29].

The comparative aspect of this research is particularly important as it aims to evaluate CZF and NZF in terms of specific capacitance, cycling stability, and impedance. It will not only determine which material outperforms the other but also shed light on the trade-offs between them. The choice of electrode material is a critical decision for supercapacitor design, and a thorough comparative analysis will guide researchers and engineers in selecting the most suitable material for their specific requirements[27].

The literature reviewed thus far underscores the potential of both CZF and NZF as promising electrode materials, each with its unique advantages. However, understanding

how these materials compare to traditional choices and to each other is essential for informed material selection and the successful development of high-performance supercapacitors.

2.9 Challenges and Future Directions

The challenges in the research on cobalt and nickel-substituted zinc ferrites revolve around achieving a balance between specific capacitance and cycling stability. The choice of substitution ratio is critical, as excessive substitution can lead to decreased cycling stability, while insufficient substitution may limit specific capacitance. The optimization of these parameters remains a challenge and requires a deep understanding of the materials' electrochemical behavior[30].

Additionally, the environmental impact and sustainability of these materials are important considerations in the context of modern energy storage systems. Researchers are increasingly focused on developing environmentally friendly electrode materials with minimal environmental footprint. Future directions in this area should explore the development of sustainable synthesis methods and the use of eco-friendly precursors[31].

Moreover, future research should aim to explore novel synthesis routes and advanced characterization techniques that can further enhance the performance of cobalt and nickel-substituted zinc ferrites. Incorporating nanoscale engineering and other innovative approaches may lead to breakthroughs in material design and energy storage technology.

The reviewed literature has highlighted the significance of supercapacitors in various applications, emphasizing their importance in energy storage and delivery. Electrode materials are central to supercapacitor performance, and optimizing these materials is essential for advancing the technology.

Zinc ferrites, both cobalt and nickel-substituted, have shown promise as electrode materials, with the potential to outperform traditional choices in terms of specific capacitance and cycling stability. However, a comprehensive comparative study that directly compares these materials and assesses their performance in practical

supercapacitor applications is currently lacking. The forthcoming research aims to address this gap and provide valuable insights into material selection for energy storage systems[32].

2.10 Research Gap and Rationale

The research gap identified in the existing literature is the absence of a comprehensive comparative study between cobalt and nickel-substituted zinc ferrites for supercapacitor applications. While individual studies have explored the electrochemical behavior of these materials, a direct comparison that considers factors such as specific capacitance, cycling stability, and impedance is necessary. This gap is significant because it impedes researchers and engineers from making informed decisions about which material is best suited for specific supercapacitor applications.

The rationale for this comparative study is rooted in the need for a systematic evaluation of these materials' performance. Such a study can provide insights into their strengths and weaknesses, ultimately aiding in material selection and the design of high-performance supercapacitors. Additionally, understanding how cobalt and nickel substitution affects these materials' electrochemical behavior can contribute to the broader knowledge of electrode materials for energy storage applications.

CHAPTER 3: MATERIALS AND METHODS

3.1 Techniques for Synthesis of Nanomaterials

The synthesis of nanomaterials represents a pivotal aspect of nanotechnology, influencing the properties and performance of materials in various applications. Numerous techniques have been developed for the synthesis of nanomaterials, each offering unique advantages and limitations. This section provides an in-depth exploration of common techniques, categorized as top-down and bottom-up approaches[33].

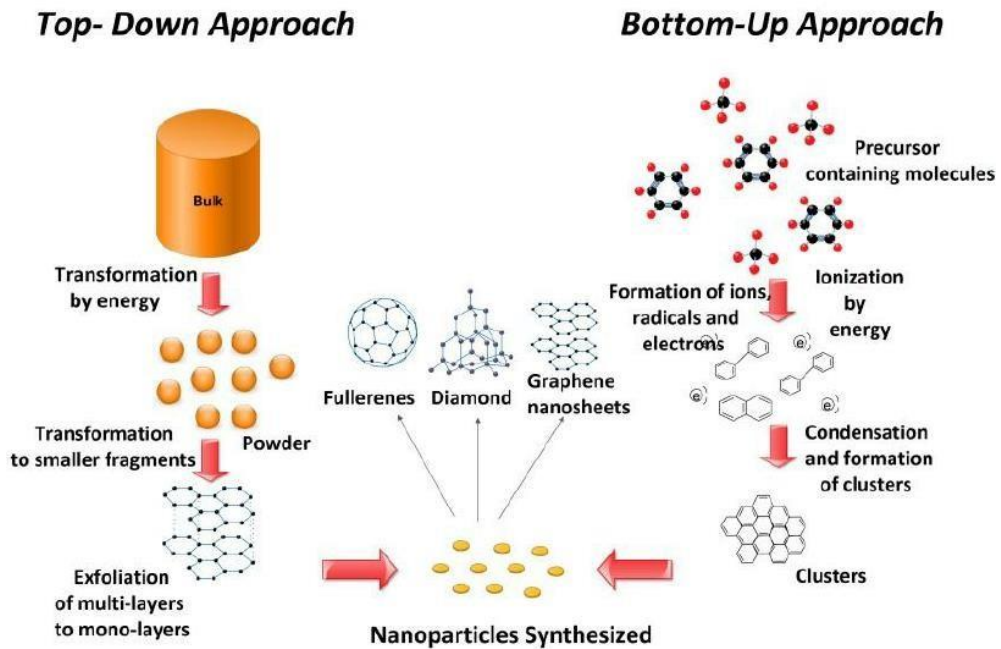


Figure 3.1: Top down and bottom-up approaches

3.2 Top-Down Approaches

Top-down approaches involve the transformation of bulk materials into nanoscale structures through mechanical, chemical, or physical means. These methods provide controlled size reduction and include:

3.2.1 Mechanical Milling

Mechanical milling, a widely employed technique, relies on the mechanical reduction of bulk materials into fine powders. This is achieved through the use of mechanical forces such as ball milling or attrition milling.

During milling, materials undergo repeated collisions, leading to particle size reduction. This approach is effective for producing nanoscale powders and is adaptable for various materials, including metals, ceramics, and polymers[34].

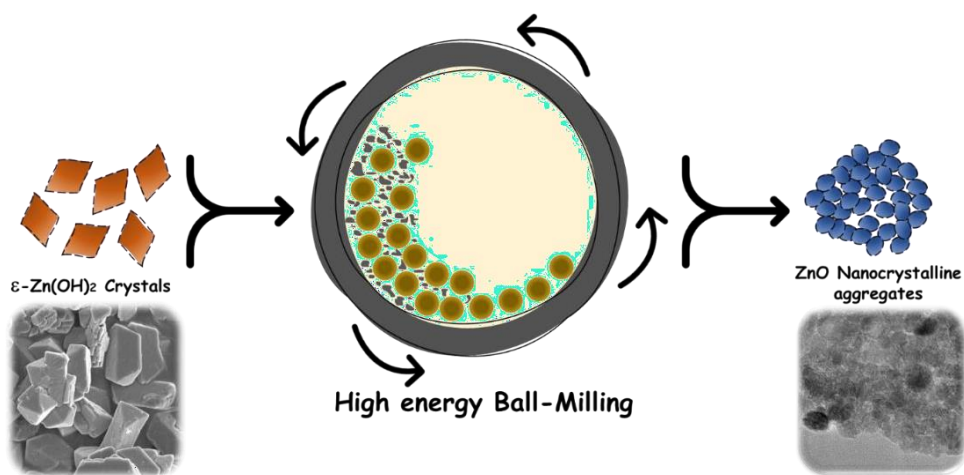


Figure 3.2: Principle of mechanical milling

3.2.2 Laser Ablation

Laser ablation involves the use of high-energy laser pulses to remove material from a target surface, resulting in the formation of nanoparticles. In this process, the high-intensity laser beam vaporizes the material, generating a plume of vapor and nanoparticles in a gas or liquid environment.

Laser ablation is particularly suited for producing nanoparticles of metals, semiconductors, and complex materials like carbon nanotubes. Its advantage lies in the ability to synthesize nanoparticles without the need for chemical precursors.[35]

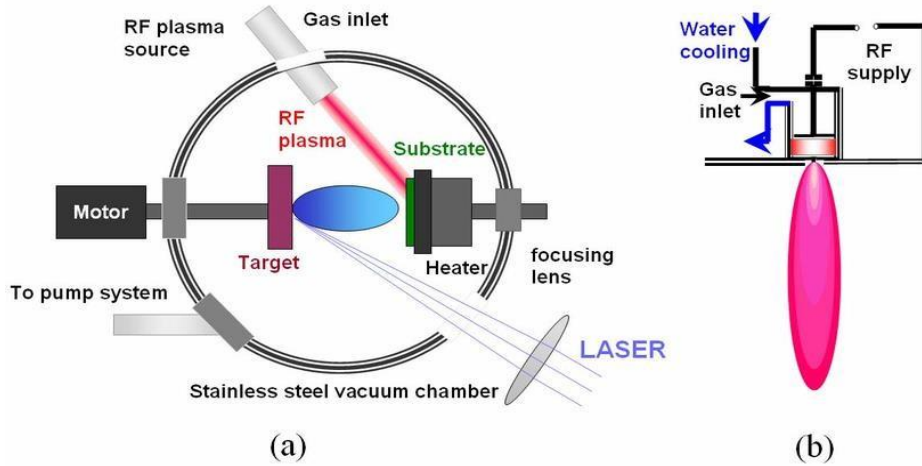


Figure 3.3: Working principle of Laser Ablation

3.3 Bottom-Up Approaches

Bottom-up approaches involve the assembly of atoms or molecules to construct nanomaterials from the ground up. These methods offer precise control over the size and structure of nanoparticles and include:

3.3.1 Sol-Gel Method

The sol-gel method is a versatile technique for synthesizing nanomaterials, particularly metal oxides. It begins with the hydrolysis and condensation of metal alkoxides or metal chlorides in a solution, forming a colloidal suspension known as a sol.

By meticulously controlling reaction parameters such as pH and temperature, nanoparticles are synthesized. Subsequent gelation and drying processes lead to the formation of nanoscale powders, thin films, or even monolithic structures.

The sol-gel method is renowned for its ability to produce high-purity materials with precise control over particle size and morphology[36].

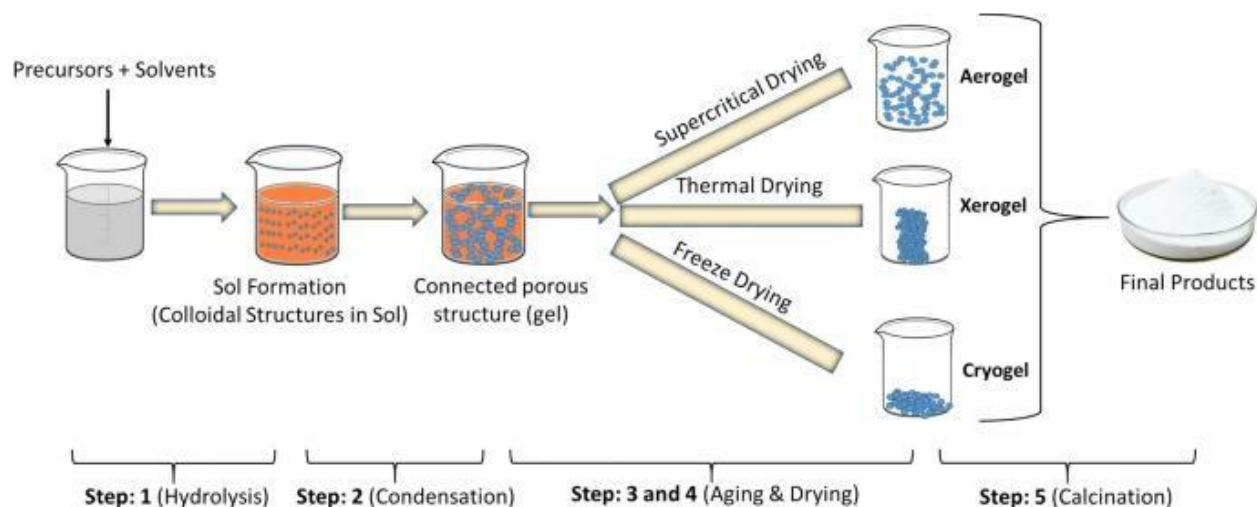


Figure 3.4: Steps involved in Sol Gel Method

3.3.2 Micro Emulsion

Micro emulsion is a technique that leverages the use of immiscible liquids, typically oil and water, stabilized by surfactants. Within this system, nanomaterials are synthesized within the confined spaces of microdroplets in the emulsion. By carefully selecting surfactants and adjusting reaction conditions, researchers can obtain nanomaterials with controlled sizes and shapes. Micro emulsion is particularly effective for producing nano catalysts, semiconductor nanoparticles, and drug delivery systems. It offers advantages in terms of monodispersity and homogeneity of nanoparticle size[37].

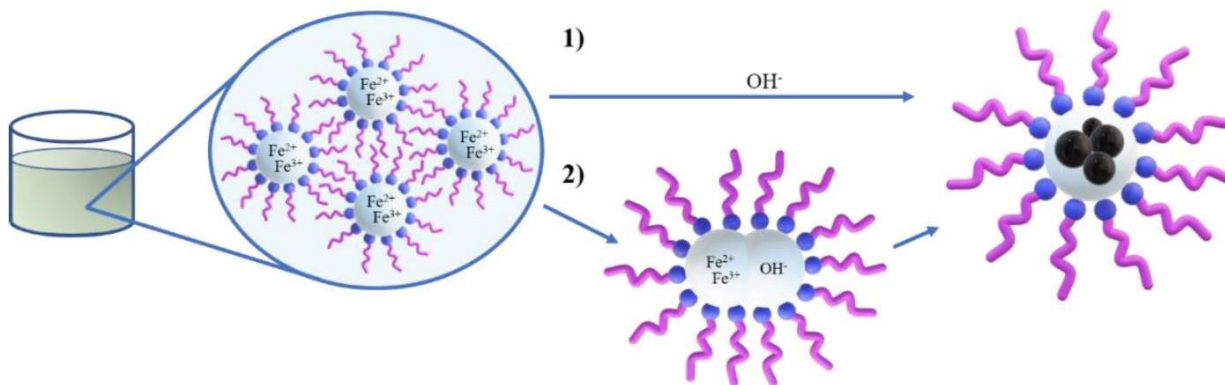


Figure 3.5: Microemulsion technique for nanoparticle synthesis

3.3.3 Solvothermal or Hydrothermal

Solvothermal and hydrothermal methods involve the synthesis of nanomaterials in high-temperature, high-pressure aqueous environments. These methods are highly advantageous for the preparation of metal oxides and inorganic nanomaterials. Solvothermal reactions occur in organic solvents, while hydrothermal reactions take place in water. The combination of elevated temperature and pressure facilitates the formation of crystalline nanoparticles with controlled properties. These methods are widely used for producing ferrites and other oxide-based nanomaterials, as they enable the precise tuning of size, morphology, and crystallinity[38].

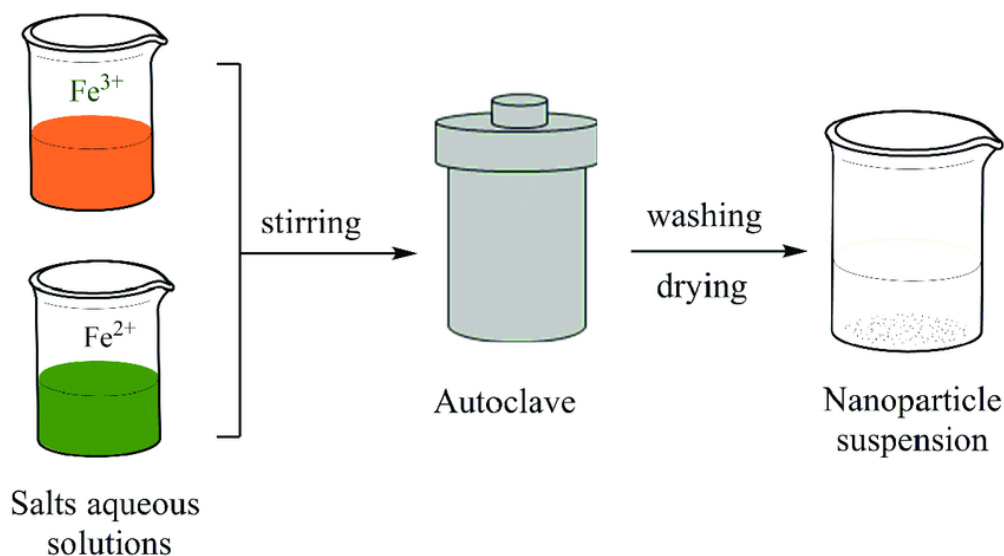


Figure 3.6: Hydrothermal synthesis of Nanoparticles

3.3.4 Chemical Co-Precipitation

Chemical co-precipitation is a straightforward yet effective method for synthesizing nanomaterials. It involves the mixing of two or more precursor solutions containing the desired ions. The addition of a precipitating agent initiates the simultaneous precipitation of the ions, leading to the formation of nanoscale particles. This technique offers control over the chemical composition and properties of nanoparticles, making it suitable for producing magnetic nanoparticles, including ferrites, for a variety of

applications. The simplicity and scalability of this method have contributed to its widespread use in nanomaterial synthesis[39].

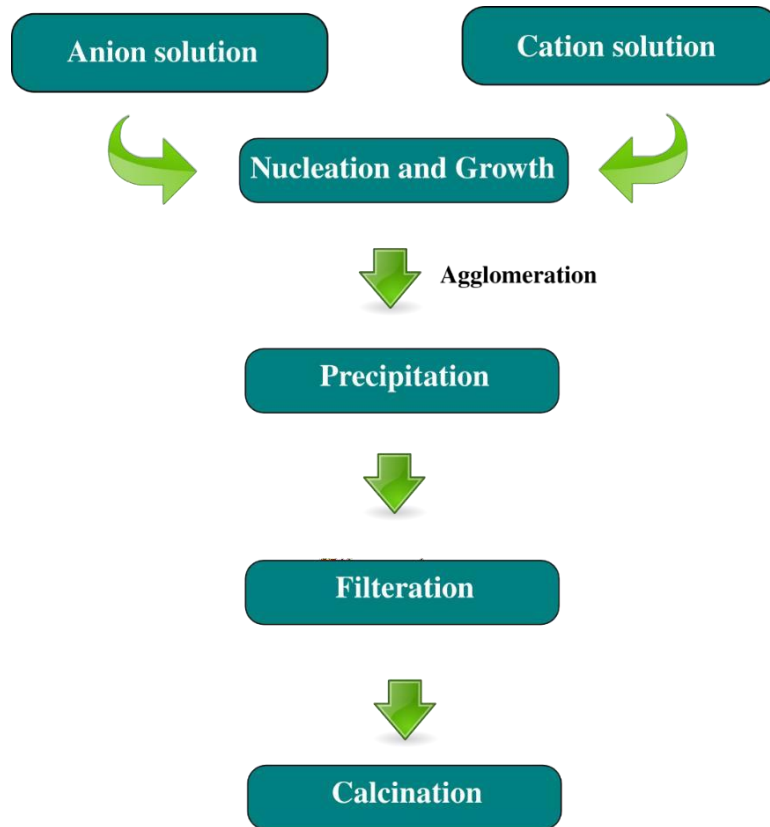


Figure 3.7: Coprecipitation Method Synthesis Nanoparticles

3.4 Synthesis of ZnFe₂O₄ Magnetic Nanoparticles

The synthesis of magnetic nanoparticles of ZnFe₂O₄ was accomplished using the co-precipitation method, a widely employed technique for producing nanoparticles with controlled properties. The process began by preparing a precursor solution. In this step, 16.00 grams of iron (III) nitrate nonahydrate (Fe (NO₃)₃·9H₂O) and 2.97 grams of zinc (II) nitrate tetrahydrate (Zn (NO₃)₂·4H₂O) were meticulously dissolved in 200 milliliters of deionized water.

To initiate the co-precipitation reaction, sodium hydroxide (NaOH) was gradually added to the precursor solution with continuous and vigorous stirring. This addition of NaOH led to a progressive increase in pH, eventually reaching a level of 13. The reaction

was carried out under these controlled conditions for a duration of 1 hour, maintaining a constant temperature of 80°C.

Upon completion of the reaction, the resulting magnetic nanoparticles were allowed to cool. Subsequently, they underwent thorough washing with deionized water and ethanol in order to remove any impurities or residual reactants. This purification process ensured the attainment of highly pure ZnFe_2O_4 nanoparticles.

The final step in the synthesis process involved sintering the purified nanoparticles at a temperature of 800°C for a duration of 3 hours. This high-temperature treatment is critical for the consolidation of nanoparticles, facilitating crystal growth and enhancing the material's overall properties.

3.5 Synthesis of $\text{Zn}_{0.5}\text{Ni}_{0.5}\text{Fe}_2\text{O}_4$ and $\text{Zn}_{0.5}\text{Co}_{0.5}\text{Fe}_2\text{O}_4$ Nanoparticles

The synthesis of substituted Zinc nano ferrites, namely $\text{Zn}_{0.5}\text{Ni}_{0.5}\text{Fe}_2\text{O}_4$ and $\text{Zn}_{0.5}\text{Co}_{0.5}\text{Fe}_2\text{O}_4$, followed a similar co-precipitation approach. However, in this case, divalent metal cations, specifically nickel (Ni) and cobalt (Co), were incorporated into the crystal structure.

For the synthesis of $\text{Zn}_{0.5}\text{Ni}_{0.5}\text{Fe}_2\text{O}_4$, 2.90 grams of nickel (II) nitrate hexahydrate ($\text{Ni}(\text{NO}_3)_2 \cdot 6\text{H}_2\text{O}$) was included in the precursor solution. Similarly, for $\text{Zn}_{0.5}\text{Co}_{0.5}\text{Fe}_2\text{O}_4$, 2.91 grams of cobalt (II) nitrate hexahydrate ($\text{Co}(\text{NO}_3)_2 \cdot 6\text{H}_2\text{O}$) was added. The remainder of the co-precipitation method mirrored the process employed for ZnFe_2O_4 , including the gradual addition of NaOH, maintaining the pH at 13, and conducting the reaction for 1 hour at a constant temperature of 80°C.

Upon the completion of the co-precipitation reaction, the resulting $\text{Zn}_{0.5}\text{Ni}_{0.5}\text{Fe}_2\text{O}_4$ and $\text{Zn}_{0.5}\text{Co}_{0.5}\text{Fe}_2\text{O}_4$ nanoparticles were subjected to the same purification steps involving multiple washes with deionized water and ethanol. This thorough purification process ensured that the substituted nanoparticles were of high purity.

As with ZnFe_2O_4 , the final step for $\text{Zn}_{0.5}\text{Ni}_{0.5}\text{Fe}_2\text{O}_4$ and $\text{Zn}_{0.5}\text{Co}_{0.5}\text{Fe}_2\text{O}_4$ synthesis involved sintering the purified nanoparticles. They were heated to 800°C and maintained

at this temperature for a duration of 3 hours. This post-synthesis sintering process allowed for further crystallization and optimization of the nanoparticles' properties, making them suitable for subsequent characterization and analysis.

These synthesized materials, ZnFe_2O_4 , $\text{Zn}_{0.5}\text{Ni}_{0.5}\text{Fe}_2\text{O}_4$ and $\text{Zn}_{0.5}\text{Co}_{0.5}\text{Fe}_2\text{O}_4$, are essential components for further characterization and analysis in various applications, including their potential use as electrode materials in supercapacitors.

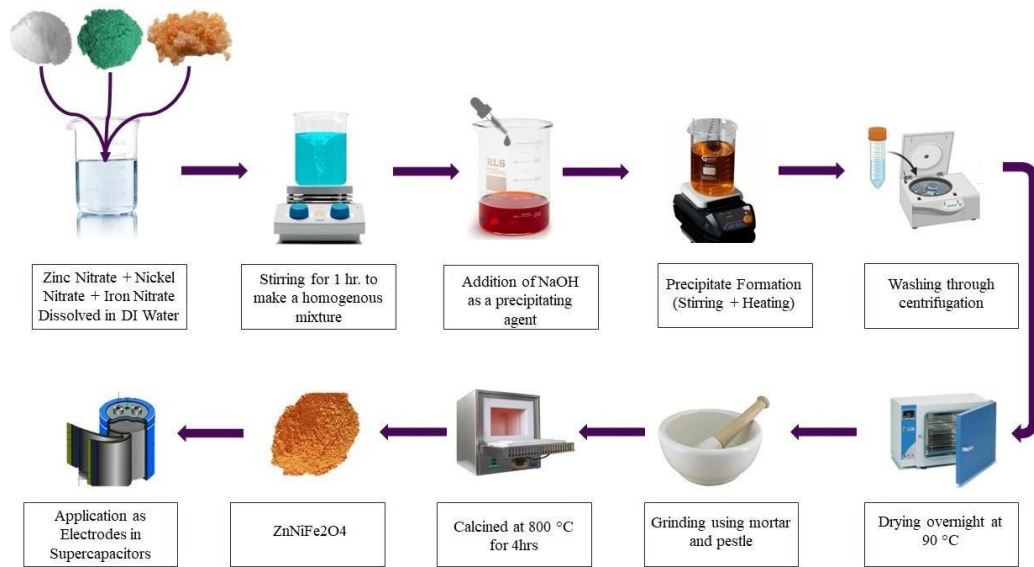


Figure 3.8: Schematic diagram of the synthesis of ZnFe_2O_4 , $\text{Zn}_{0.5}\text{Ni}_{0.5}\text{Fe}_2\text{O}_4$ and $\text{Zn}_{0.5}\text{Co}_{0.5}\text{Fe}_2\text{O}_4$

CHAPTER 4: CHARACTERIZATION

4.1 X-Ray Diffraction techniques

4.1.1 Principle:

X-ray diffraction (XRD) is a fundamental characterization technique used to investigate the crystal structure and crystallinity of materials. It operates on the principles of Bragg's law, where X-rays are directed onto a crystal lattice, and the resultant diffracted X-rays create patterns that unveil information about lattice spacing and crystal arrangement[40].

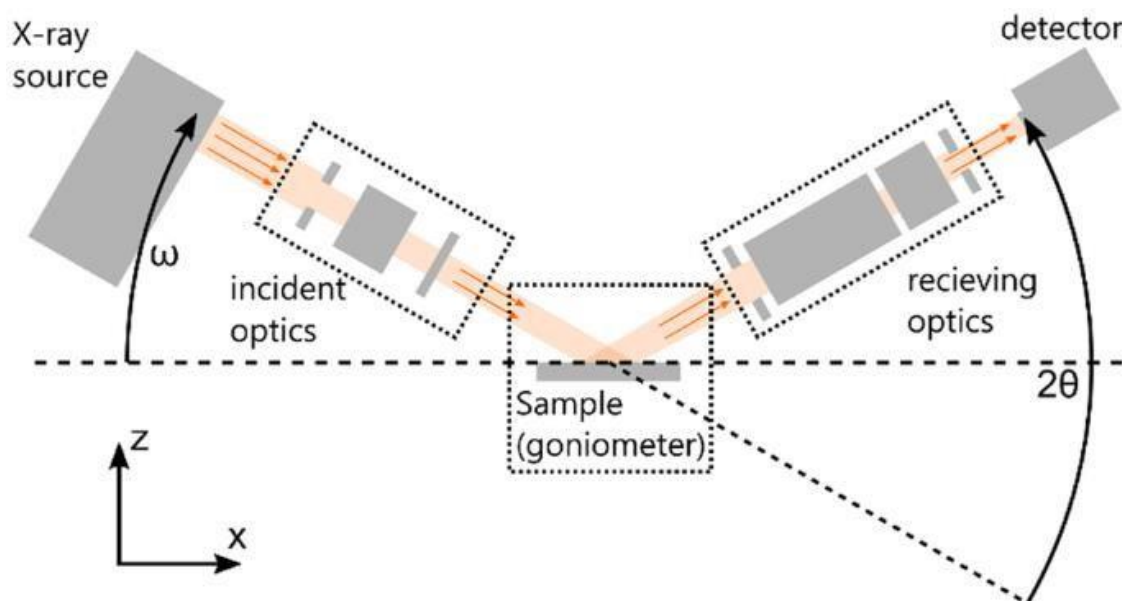


Figure 4.1: Working principle of XRD

4.1.2 Relevance to Research:

XRD plays a pivotal role in characterizing the structural properties of the synthesized materials, specifically ZnFe_2O_4 , $\text{ZnNiFe}_2\text{O}_4$, and $\text{ZnCoFe}_2\text{O}_4$. It provides crucial insights into crystal phases, crystallite size, and lattice parameters. By examining XRD patterns, we can not only confirm the formation of the intended spinel structure but also assess the influence of metal substitution on crystallographic characteristics. This

information is essential for understanding how the materials' structural properties may impact their electrochemical behavior[40, 41].

4.2 Scanning Electron Microscopy (SEM)

4.2.1 Principle:

Scanning Electron Microscopy (SEM) is an imaging technique that employs a focused beam of electrons to scan the surface of a specimen. Secondary electrons emitted from the surface are collected to create detailed, high-resolution images of the sample's morphology[41].

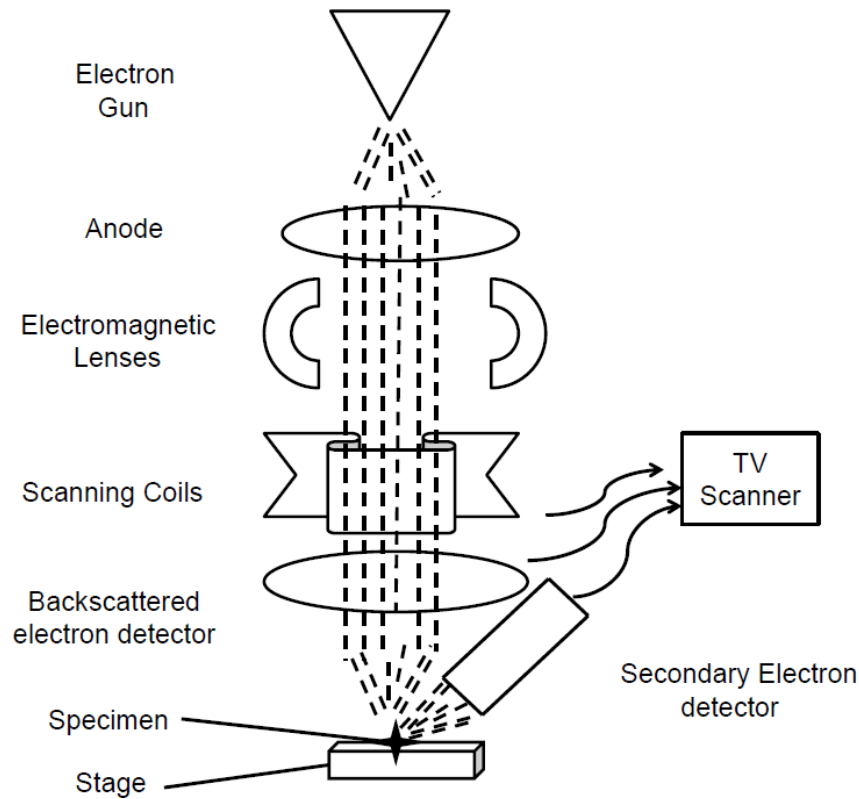


Figure 4.2: Working principle of Scanning Electron Microscope

4.2.2 Relevance to Research:

SEM is instrumental in visualizing the surface morphology, size, and shape of nanoparticles. It offers valuable insights into particle distribution and agglomeration,

aiding in confirming the nanoscale nature of the synthesized materials. SEM also helps assess the effect of metal substitution on particle morphology. By providing a visual representation of the materials' surface features, SEM contributes significantly to the overall characterization process[41].

4.3 Fourier Transform Infrared Spectroscopy (FTIR)

4.3.1 Principle:

Fourier Transform Infrared Spectroscopy (FTIR) is a spectroscopic technique that analyzes the vibrational modes of molecules in a sample. It operates by passing infrared radiation through the sample, with the resulting absorption or transmission spectra providing information about chemical functional groups and bonding[42].

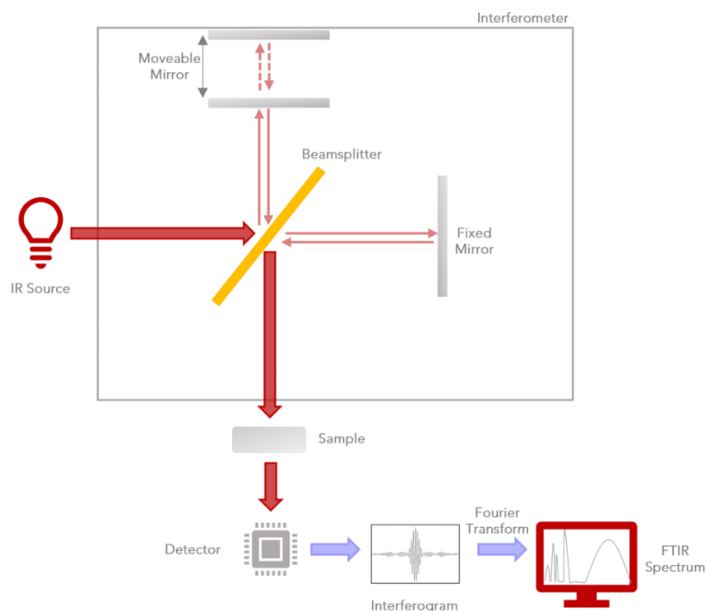


Figure 4.3: Working principle of FTIR

4.3.2 Relevance to Research:

FTIR serves as a valuable tool for identifying chemical bonds and functional groups on the surface of nanoparticles. It assists in confirming the presence of spinel structures and assessing the chemical composition of the synthesized materials. By analyzing FTIR

spectra, researchers can gain insights into how metal substitution may influence the surface chemistry of the materials, which is critical for understanding their electrochemical properties[42].

4.4 Raman Spectroscopy

4.4.1 Principle:

Raman spectroscopy is a vibrational spectroscopic technique that involves the scattering of monochromatic light by a sample. The shift in wavelength of the scattered light (Raman shift) provides information about molecular vibrations and crystal symmetry, aiding in the identification and characterization of materials[43].

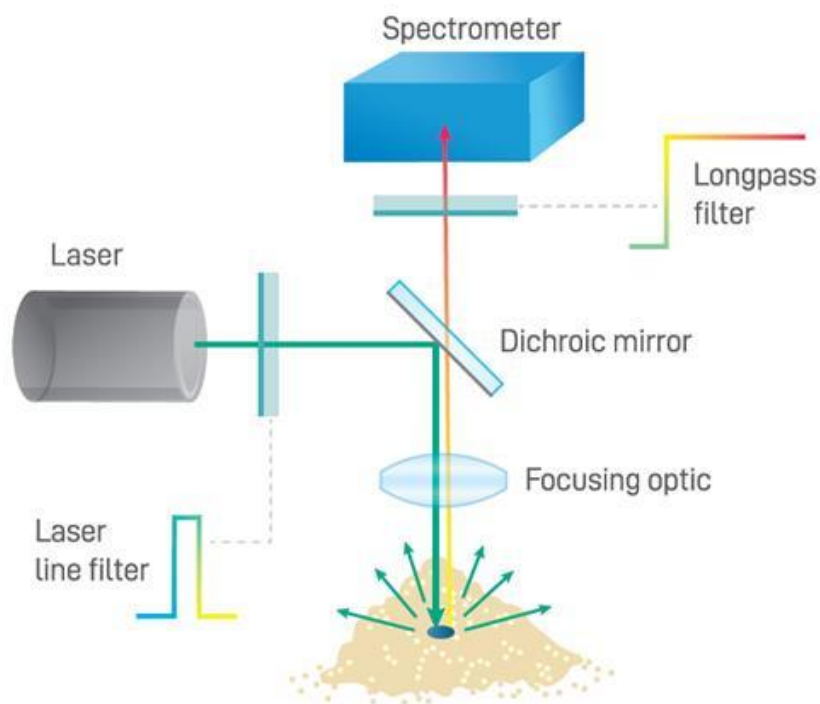


Figure 4.4: Working principle of Raman Spectroscopy

4.4.2 Relevance to Research:

Raman spectroscopy is indispensable for confirming the structural integrity and phase purity of synthesized materials. It can detect subtle changes in crystal structure and

vibrational modes induced by metal substitution. Raman analysis is particularly useful for ensuring that the desired spinel phase is maintained during the synthesis process. By probing the vibrational properties of the materials, Raman spectroscopy provides valuable insights into their structural stability[43, 44].

4.5 Dielectric Analysis

4.5.1 Principle:

Dielectric analysis involves measuring the response of a material to an applied electric field. It assesses the dielectric properties of the material, including permittivity and dielectric loss, which reflect the material's ability to store and dissipate electrical energy[44].

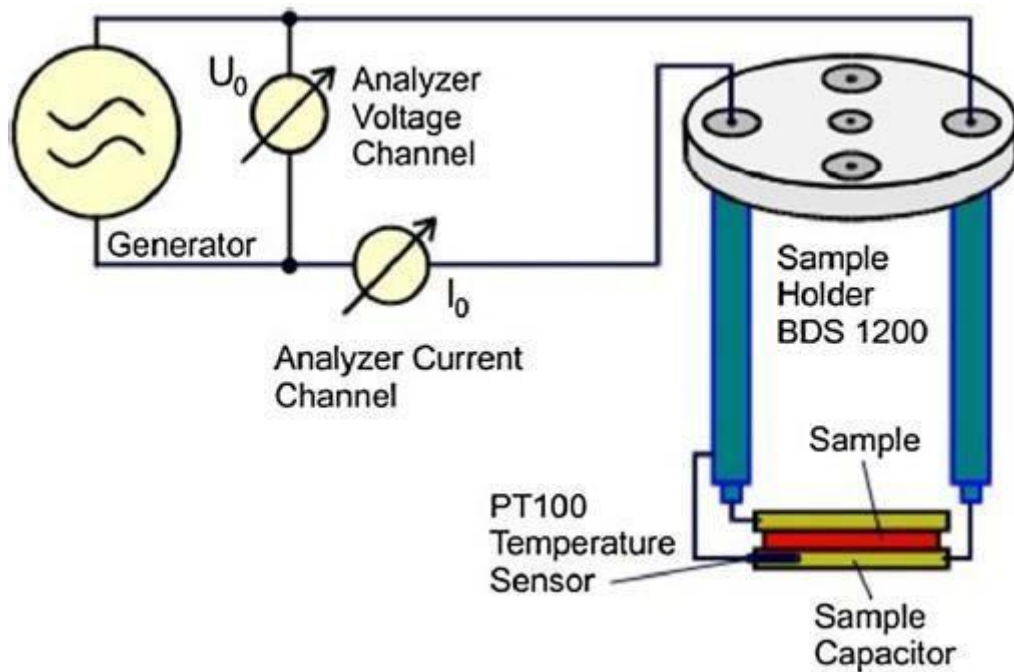


Figure 4.5: Working principle of Dielectric

4.5.2 Relevance to Research:

Dielectric analysis is of paramount importance for understanding the electrical behavior of materials, particularly in the context of supercapacitor applications. It helps

evaluate the dielectric constant and loss tangent, which are critical parameters for energy storage. By conducting dielectric analysis, researchers can assess how metal substitution influences the dielectric properties of the materials. This information is crucial for optimizing their performance as supercapacitor electrodes[44].

4.6 Cyclic Voltammetry

4.6.1 Principle:

Cyclic Voltammetry (CV) is an electrochemical technique that enables the study of redox behavior in materials. It involves cyclically varying the potential applied to an electrode and measuring the resulting current response[45].

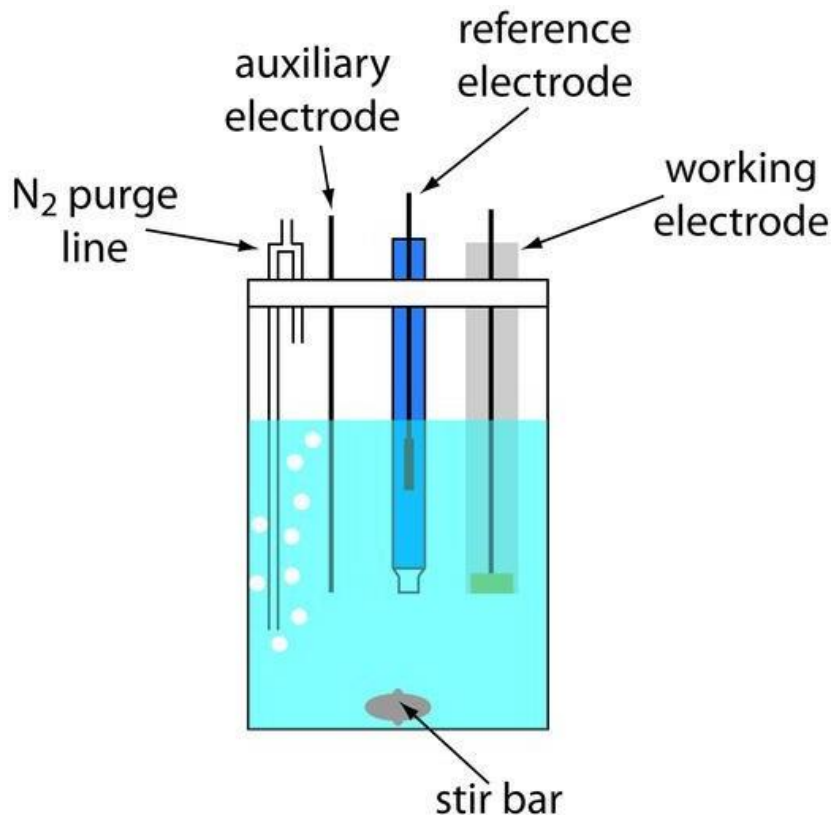


Figure 4.6: Working principle of cyclic voltammetry

4.6.2 *Relevance to Research:*

CV is an essential tool for evaluating the electrochemical performance of materials intended for use in supercapacitors. It provides insights into specific capacitance, cyclic stability, and charge/discharge behavior. By subjecting the synthesized materials to CV, researchers can assess their suitability as supercapacitor electrodes. CV data also enable the determination of critical electrochemical parameters that impact the materials' overall performance[45].

These characterization techniques collectively provide a comprehensive understanding of the structural, morphological, chemical, electrical, and electrochemical properties of the synthesized materials, namely ZnFe₂O₄, ZnNiFe₂O₄, and ZnCoFe₂O₄ nanoparticles. They are essential for validating the quality and performance of these materials and assessing their potential suitability as electrode materials for supercapacitors. These techniques empower researchers to make informed decisions regarding material selection and optimization for specific energy storage applications.

CHAPTER 5: RESULTS AND DISCUSSION

5.1 X-Ray Diffraction Spectroscopy

ZnFe₂O₄, ZnNiFe₂O₄, and ZnCoFe₂O₄ nanoparticles' XRD patterns were seen at room temperature in the 2θ ranges of 20-70 °C with Cu K radiation, as illustrated in Figure. The samples' purity may be seen from the fact that there is no impurity peak in their XRD pattern [19].

The following equation was used to calculate the lattice parameter values,

$$\sin^2 \theta = (\lambda^2/a^2)(h^2 + k^2 + l^2)$$

Where λ is the X-ray wavelength (1.540 Å), a is the lattice constant, $h k l$ are the miller indices of the reflection planes, and θ is the angle of diffraction. ZnNiFe₂O₄ has a lattice parameter value of 8.4310, ZnNiFe₂O₄ has a lattice parameter value of 8.4030, whereas ZnCoFe₂O₄ has a value of 8.4250. ZnFe₂O₄ sample crystallite size was found to be 19.26 nm, ZnNiFe₂O₄ to be 43.12 nm, and ZnCoFe₂O₄ to be 34.20 nm. Using Debye-Scherrer's formula, the diameters of the samples' crystallites were determined as follows [20]

$$t = k\lambda / (\beta \cos\theta)$$

Where λ is the X-ray wavelength, t is the crystallite size, β is the FWHM and θ is the angle of diffraction. All the structural parameters calculated from the XRD pattern are tabulated in Table 1.

The ZnFe₂O₄ sample's x-ray density was determined to be 5.42 g/cm³, ZnNiFe₂O₄'s density was 5.32 g/cm³, and ZnCoFe₂O₄'s density was 4.90 g/cm³. ZnFe₂O₄ was found to have a unit cell volume of 599.29, ZnNiFe₂O₄ of 593.34, and ZnCoFe₂O₄ of 598.01. The co-precipitation process is a great way to synthesize the necessary-sized nanoparticles, as shown by the XRD results [21].

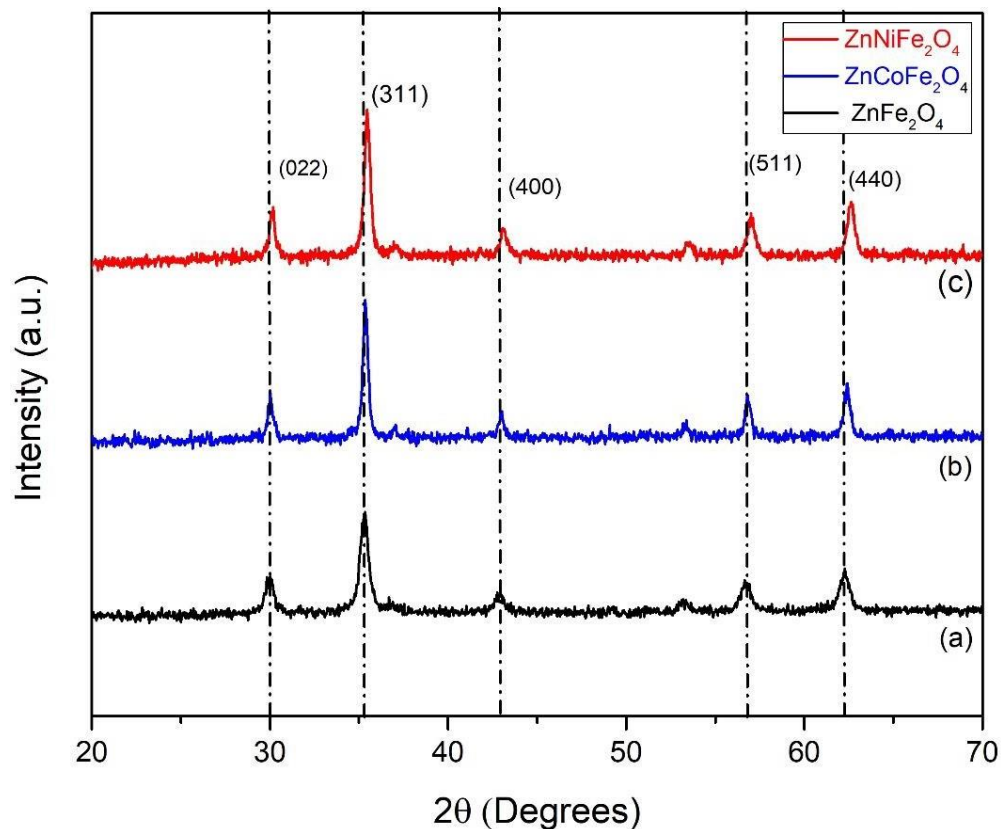


Figure 5.1: The X-Ray diffraction Pattern of ZnFe_2O_4 , $\text{Zn}_{0.5}\text{Ni}_{0.5}\text{Fe}_2\text{O}_4$ and $\text{Zn}_{0.5}\text{Co}_{0.5}\text{Fe}_2\text{O}_4$ Nanoparticles

Table 5.1: Properties of ZnFe_2O_4 , $\text{Zn}_{0.5}\text{Ni}_{0.5}\text{Fe}_2\text{O}_4$ and $\text{Zn}_{0.5}\text{Co}_{0.5}\text{Fe}_2\text{O}_4$ Nanoparticles

Sample	Lattice constant	Volume	Crystal size	Density
ZnFe_2O_4	8.4310	599.29	19.62	5.34
$\text{ZnNiFe}_2\text{O}_4$	8.4030	593.34	43.12	5.32
$\text{ZnCoFe}_2\text{O}_4$	8.4250	598.01	34.20	4.90

5.2 Scanning Electron Microscopy

All three spinel materials had a homogeneous and clearly defined morphology with spherical nanoparticles, as seen by the SEM images. The average particle size was found to be in the nanometer range, proving that nanoparticles had successfully been synthesized. The replacement of various transition metal ions was shown to affect the surface shape of the spinel nanoparticles. According to the SEM images, ZnFe_2O_4 nanoparticles are spherical in form and range in size from 20 to 30 nm. The nanoparticles' surfaces are uniformly smooth. While the typical size of $\text{ZnNiFe}_2\text{O}_4$ and $\text{ZnCoFe}_2\text{O}_4$ nanoparticles is 30 to 40 nm, they are also spherical in form. [5]

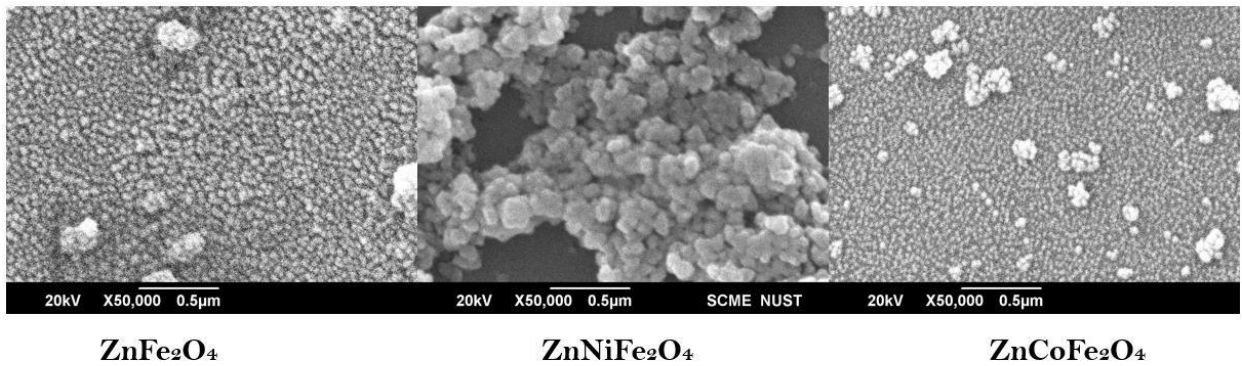


Figure 5.2: SEM images of ZnFe_2O_4 , $\text{Zn}_{0.5}\text{Ni}_{0.5}\text{Fe}_2\text{O}_4$ and $\text{Zn}_{0.5}\text{Co}_{0.5}\text{Fe}_2\text{O}_4$ Nanoparticles

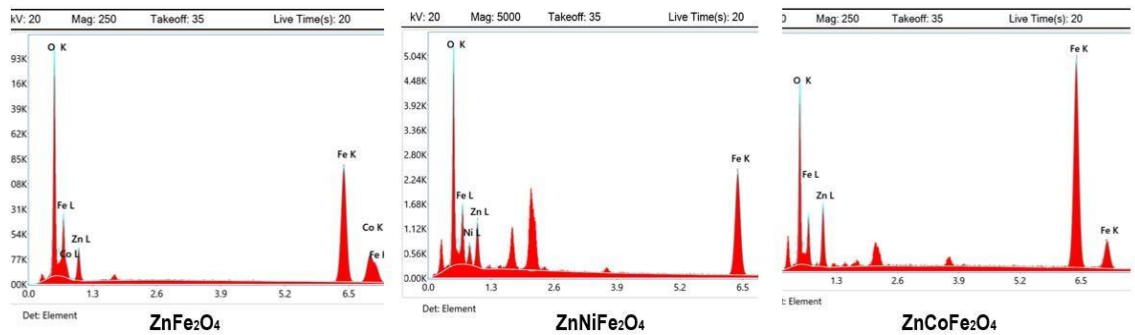


Figure 5.3: EDS spectrum of ZnFe_2O_4 , $\text{Zn}_{0.5}\text{Ni}_{0.5}\text{Fe}_2\text{O}_4$ and $\text{Zn}_{0.5}\text{Co}_{0.5}\text{Fe}_2\text{O}_4$ Nanoparticles

Additionally, the SEM study shed light on the nanoparticles' accumulation behavior. Different agglomeration levels were seen in the spinel materials, indicating

various interparticle interactions brought on by the presence of various transition metal ions.[22]

The EDS spectra obtained from the spinel nanoparticles confirmed the presence of zinc (Zn), iron (Fe), nickel (Ni), and cobalt (Co) elements in their respective compositions. The relative elemental ratios were calculated, indicating the successful incorporation of the transition metal ions into the spinel lattice. The quantitative analysis also revealed the stoichiometric ratios of the elements in the spinel structures. The results of SEM show that all three types of nanoparticles have a similar morphology [22].

5.3 Raman Spectroscopy

In this study, the Raman spectra of three distinct ferrite samples—Zinc Ferrite, Zinc Cobalt Ferrite, and Zinc Nickel Ferrite—have been comprehensively analyzed, yielding insightful findings that shed light on their unique vibrational characteristics and enabling their differentiation.

The acquired spectra unveil a series of five prominent peaks, each of which carries distinct vibrational significance within the crystal lattice and ion arrangements of the samples under investigation.

The first discernible peak, located at approximately 650 cm^{-1} , corresponds to the A_{1g} mode. This vibrational mode is attributed to the motion of Fe^{3+} ions within the octahedral coordination sites within the lattice structure. A subsequent peak, situated around 540 cm^{-1} , is assigned to the E_g mode. This mode is closely associated with the vibration of Fe^{3+} ions occupying tetrahedral coordination sites.

The third peak, positioned at approximately 490 cm^{-1} , is indicative of the F_{2g} (1) mode, signifying the vibrational behavior of Zn^{2+} ions within tetrahedral coordination sites. The fourth peak, situated near 390 cm^{-1} , represents the F_{2g} (2) mode, reflecting the vibration of Zn^{2+} ions within octahedral coordination sites. Lastly, the fifth peak, occurring at approximately 280 cm^{-1} , corresponds to the F_{2g} (3) mode, elucidating the vibration of O^{2-} ions. [23]

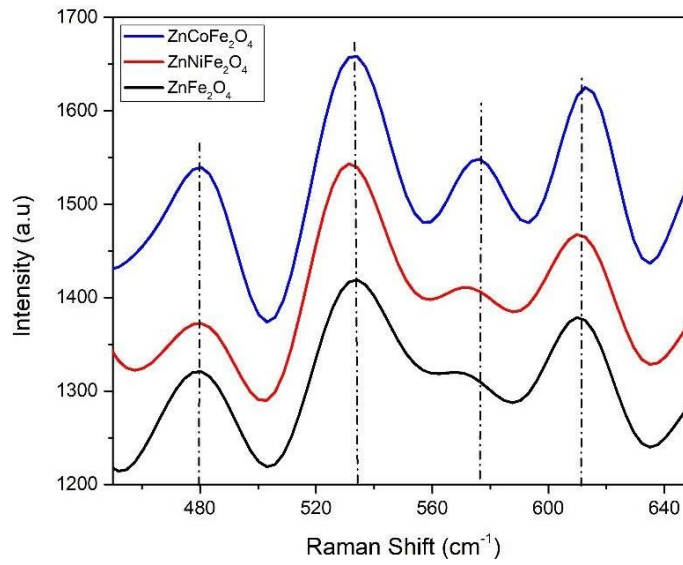


Figure 5.4: Raman Shift of ZnFe₂O₄, ZnNiFe₂O₄ and ZnCoFe₂O₄ Nanoparticles

intensities of these peaks offer a discerning characteristic for distinguishing among the three samples. In the Zinc Ferrite sample, the A_{1g} mode exhibits the highest intensity, succeeded by the Zinc Cobalt Ferrite sample, and finally the Zinc Nickel Ferrite sample.

In contrast, the E_g mode attains its greatest intensity in the Zinc Cobalt Ferrite sample, followed by the Zinc Ferrite sample, and the Zinc Nickel Ferrite sample. Similarly, the F_{2g}(1) mode's most pronounced intensity is observed in the Zinc Nickel Ferrite sample, followed by the Zinc Cobalt Ferrite sample, and the Zinc Ferrite sample. [24]

Furthermore, the shifts in peak positions offer additional avenues for differentiation. Notably, the Zinc Cobalt Ferrite sample displays the lowest frequency for the A_{1g} mode, followed by the Zinc Ferrite sample, and the Zinc Nickel Ferrite sample. This is attributed to the higher mass of cobalt ions, which results in a correspondingly lower frequency vibration. Analogously, the Zinc Nickel Ferrite sample manifests the lowest frequency for the E_g mode, followed by the Zinc Cobalt Ferrite sample, and the Zinc Ferrite sample. This outcome aligns with the greater mass of nickel ions, contributing to the observed lower frequency vibration.

The implications of these results are profound and extend to the ensuing discussion. The distinct peak intensities and shifts in peak positions effectively differentiate among Zinc Ferrite, Zinc Cobalt Ferrite, and Zinc Nickel Ferrite samples. This discrimination is rooted in the intricate interplay between ion masses and lattice vibrations, underscoring the vital role of these factors in determining the distinctive Raman signatures of the investigated ferrites.

The Zinc Ferrite sample's unique A_{1g} mode intensity reflects the lower mass of zinc ions relative to cobalt and nickel ions. Conversely, the heightened E_g mode intensity in the Zinc Cobalt Ferrite sample results from the lower mass of cobalt ions. Additionally, the predominant intensity of the F_{2g}(1) mode in the Zinc Nickel Ferrite sample is attributed to the greater mass of nickel ions. These distinctive peak positions further accentuate the differentiation potential. Notably, the shift in the A_{1g} mode frequency aligns with the cobalt ion's higher mass, thus inducing a lower frequency vibration. Likewise, the lower frequency of the E_g mode in the Zinc Nickel Ferrite sample can be attributed to the increased mass of nickel ions. [5, 25]

The Raman spectroscopy study of zinc ferrite, zinc cobalt ferrite, and zinc nickel ferrite can be used to understand their structure and properties for supercapacitor electrodes. The high intensity of the A_{1g} mode in the Raman spectra of zinc ferrite indicates that it has a high electrical conductivity, which is important for supercapacitor electrodes.

The low frequency of the A_{1g} mode in the Raman spectra of zinc cobalt ferrite indicates that it has a higher energy density than zinc ferrite, which is also important for supercapacitor electrodes. These results can be used to optimize the structure and properties of these materials for use as supercapacitor electrodes.

5.4 Fourier-Transform Infrared Spectroscopy

The obtained FTIR spectra from the distinct ferrite samples—Zinc Ferrite, Zinc Cobalt Ferrite, and Zinc Nickel Ferrite—reveal distinct features characterized by three

primary peaks, each providing unique insights into the vibrational behavior of chemical bonds within the samples.

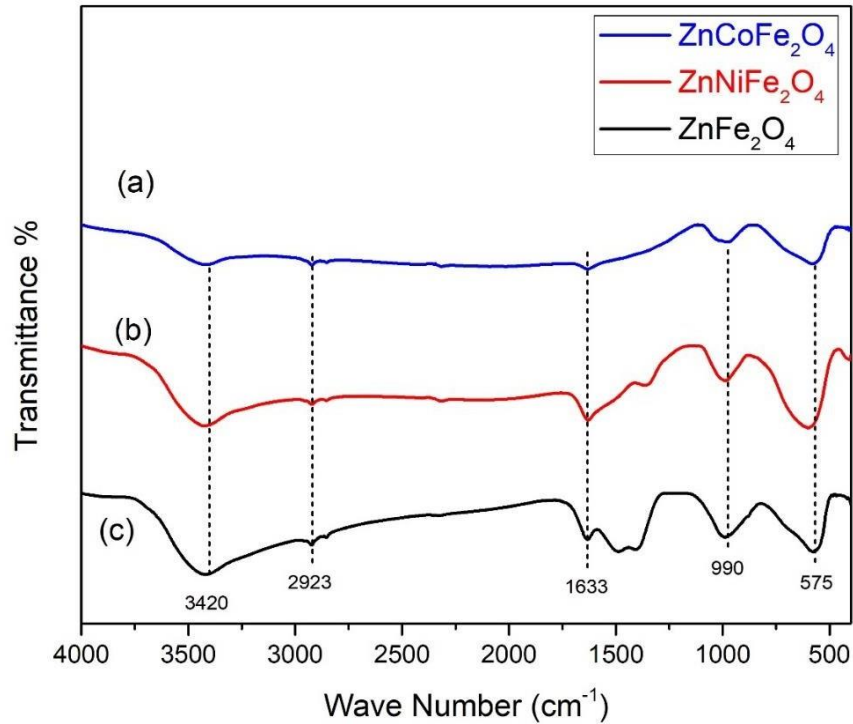


Figure 5.5: The X-Ray diffraction Pattern of ZnFe₂O₄, Zn_{0.5}Ni_{0.5}Fe₂O₄ and Zn_{0.5}Co_{0.5}Fe₂O₄ Nanoparticles

Firstly, a notable peak positioned at approximately 3420 cm⁻¹ signifies the stretching vibration of O-H bonds present in water molecules. This common peak is observed consistently across all three samples, attributed to their exposure to ambient air before measurement.

A significant peak around 1633 cm⁻¹ is ascribed to the stretching vibration of Fe-O bonds in the tetrahedral sites of the lattice structure. This peak's frequency subtly differs among the samples, being slightly higher in Zinc Cobalt Ferrite and Zinc Nickel Ferrite compared to Zinc Ferrite. This disparity implies enhanced Fe-O bond strength in the former samples due to the greater valence electronegativity of cobalt and nickel ions, resulting in a stronger attraction of oxygen atoms.

Furthermore, a peak around 990 cm^{-1} corresponds to the bending vibration of Fe-O bonds within the octahedral sites. Analogously, this peak appears at slightly elevated frequencies in Zinc Cobalt Ferrite and Zinc Nickel Ferrite, attributed once again to the augmented bonding strength facilitated by cobalt and nickel ions. [27, 28]

Concurrently, secondary peaks emerge from the spectra due to vibrations within other chemical bonds present in the ferrites, involving Zn-O and Co-O bonds.

When we carefully look at the spectra, we notice that they are quite similar. This is because all three samples share a basic structure called a spinel. The main difference is in the tiny spaces within the structure where metal ions sit. In Zinc Ferrite, only zinc ions are in these spaces, while in Zinc Cobalt Ferrite and Zinc Nickel Ferrite, there's a mix of zinc and cobalt or zinc and nickel ions. [29]

This difference in the metal ions in these spaces affects how strong certain bonds are between iron (Fe) and oxygen (O) atoms. This, in turn, affects the heights of the peaks we see in the FTIR measurements. That's why we see slightly higher peaks in Zinc Cobalt Ferrite and Zinc Nickel Ferrite compared to Zinc Ferrite. It's like a small bump in the music of the spectra.

To put it simply, even though the spectra look alike, the types of metal ions in the structure cause some vibrations to be a bit stronger, making those peaks a bit taller in Zinc Cobalt Ferrite and Zinc Nickel Ferrite when compared to Zinc Ferrite. [30]

In addition, the peak centered around 600 cm^{-1} corresponds to the stretching vibration of Zn-O bonds in the tetrahedral sites. Remarkably, this peak is consistent in all three samples due to the presence of zinc ions within their respective tetrahedral sites. Slight frequency fluctuations are noticeable in Zinc Cobalt Ferrite and Zinc Nickel Ferrite, aligning with the trends detected in preceding peaks.

The higher peak frequencies observed in Zinc Cobalt Ferrite and Zinc Nickel Ferrite's spectra compared to Zinc Ferrite indicate stronger Fe-O bonds, a favorable trait for supercapacitor electrodes due to potentially higher specific capacitance. The presence of the peak around 600 cm^{-1} across all samples signifies Zn-O bonds in tetrahedral sites,

beneficial for electrochemical energy storage. The similarities in the spectra suggest these ferrites could be candidates for supercapacitor electrodes [29]

5.5 Dielectric

Fig. (a) shows the dielectric constant (ϵ') of three types of ferrites, ZnFe_2O_4 , $\text{Zn}_{0.5}\text{Ni}_{0.5}\text{Fe}_2\text{O}_4$ and $\text{Zn}_{0.5}\text{Co}_{0.5}\text{Fe}_2\text{O}_4$, as a function of frequency (Inf). Ferrites are magnetic materials that can be used for various applications, such as microwave devices, transformers, and sensors. The dielectric constant is a measure of how much a material can store electric charge in an electric field. It affects the speed and efficiency of electromagnetic waves passing through the material [34].

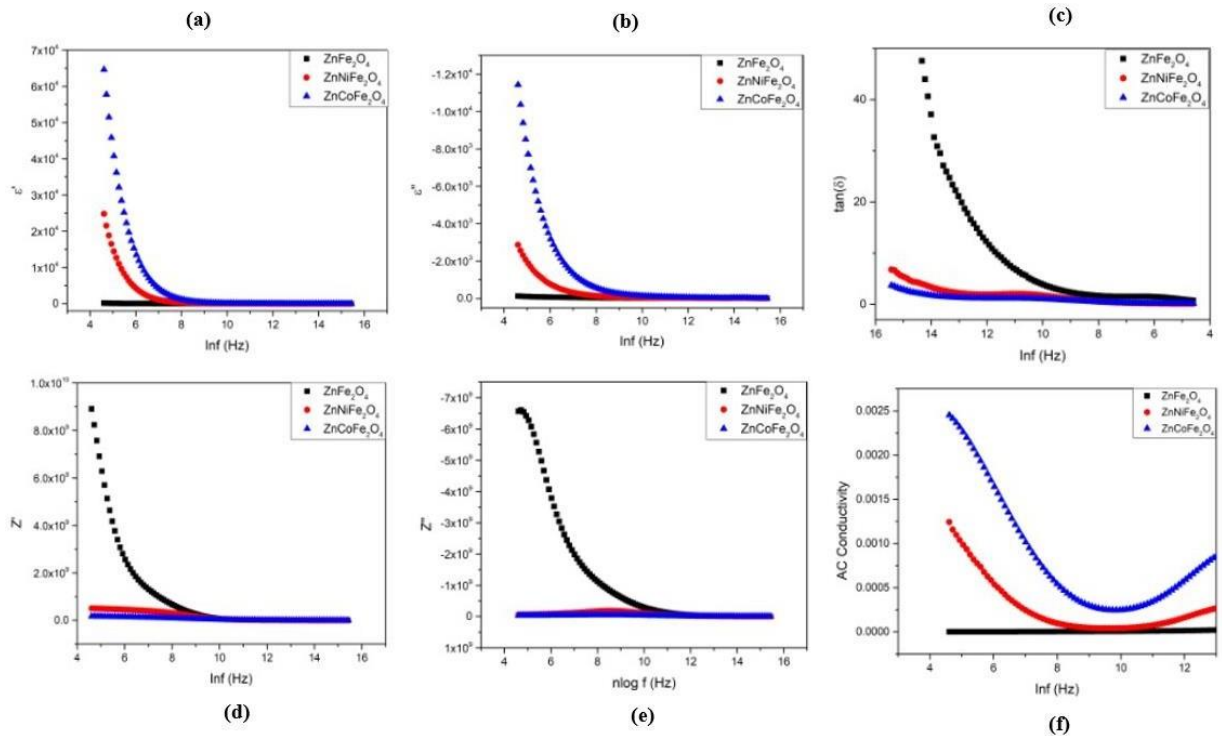


Figure 5.6: Dielectric properties of ZnFe_2O_4 , $\text{Zn}_{0.5}\text{Ni}_{0.5}\text{Fe}_2\text{O}_4$ and $\text{Zn}_{0.5}\text{Co}_{0.5}\text{Fe}_2\text{O}_4$ Nanoparticles

The graph depicts that the dielectric constant of the ferrites decreases as the frequency increases. This means that the materials become less polarizable and less responsive to the electric field at higher frequencies.

One possible reason behind the dielectric behavior of ferrites is the electron hopping mechanism. This means that the electric current in ferrites is carried by electrons that jump from one iron atom to another on the octahedral sites of the crystal structure. Iron atoms can have two different oxidation states, Fe^{2+} and Fe^{3+} , which have different numbers of electrons. When an electric field is applied, the electrons tend to move from Fe^{2+} to Fe^{3+} atoms, creating a polarization in the material. The frequency of the electric field affects the rate of electron hopping and the degree of polarization. At low frequencies, the electrons have enough time to hop and align with the field, resulting in a high dielectric constant. At high frequencies, the electrons cannot hop fast enough and lag the field, resulting in a low dielectric constant [34].

5.5.1 Imaginary part of Dielectric Permittivity

Fig. (b) of the imaginary part shows the dielectric loss of the ferrites, which is related to the energy dissipation of the material in an electric field. The dielectric loss is influenced by various factors, such as the grain size, the grain boundary, the impurities, and the defects in the material.[46]

The graph shows that ZnFe_2O_4 and $\text{Zn}_{0.5}\text{Ni}_{0.5}\text{Fe}_2\text{O}_4$ have similar dielectric loss behaviors, which decrease with increasing frequency. This may indicate that these materials have similar grain sizes and grain boundaries, and that the electron hopping mechanism is dominant in their dielectric loss. The electron hopping mechanism causes a lag between the polarization and the electric field, which results in energy dissipation. The graph also shows that $\text{Zn}_{0.5}\text{Co}_{0.5}\text{Fe}_2\text{O}_4$ has a different dielectric loss behavior, which increases with increasing frequency. This may indicate that this material has a different grain size and grain boundary, and that another mechanism is involved in its dielectric loss [35].

5.5.2 Dielectric Loss

Fig. (c) shows the tangent of the dielectric loss angle $\tan(\delta)$ of the ferrites as a function of frequency ($\ln f$). The dielectric loss angle is a measure of how much energy is

dissipated as heat when an alternating electric field is applied to a material. It is related to the phase difference between the electric field and the polarization of the material [36].

The graph shows that ZnFe_2O_4 has a high $\tan(\delta)$ at low frequencies, which means that it has a high dielectric loss and a large phase difference between the electric field and the polarization. This may be due to the presence of impurities or defects in the material that cause charge trapping and leakage currents. The graph also shows that ZnFe_2O_4 has a low $\tan(\delta)$ at high frequencies, which means that it has a low dielectric loss and a small phase difference between the electric field and the polarization. This may be due to the electron hopping mechanism, which becomes faster and more efficient at high frequencies, reducing the energy dissipation [39].

The graph shows that $\text{Zn}_{0.5}\text{Ni}_{0.5}\text{Fe}_2\text{O}_4$ and $\text{Zn}_{0.5}\text{Co}_{0.5}\text{Fe}_2\text{O}_4$ have similar $\tan(\delta)$ behaviors, which increase with increasing frequency. This means that they have increasing dielectric loss and phase difference between the electric field and the polarization. This may be due to the Maxwell-Wagner relaxation, which becomes more significant at high frequencies, causing charge accumulation and polarization reversal at the grain boundaries [40].

5.5.3 Real part of Impedance

Fig. (d) shows the real part of impedance (Z') of the ferrites as a function of frequency (Inf). Impedance is a measure of how much a material resists the flow of alternating current. It is related to the resistance and the reactance of the material [39]. The graph shows that ZnFe_2O_4 has a high impedance at low frequencies, which means that it has a high resistance and a low reactance. This may be due to the presence of impurities or defects in the material that increase the scattering and collision of charge carriers. The graph also shows that ZnFe_2O_4 has a low impedance at high frequencies, which means that it has a low resistance and a high reactance. The reactance may increase due to the inductive or capacitive effects of the material [41].

The graph shows that $\text{Zn}_{0.5}\text{Ni}_{0.5}\text{Fe}_2\text{O}_4$ and ZnCoFe_2O have similar impedance behaviors, which are almost constant with increasing frequency. This means that they have almost constant resistance and reactance.

5.5.4 *Imaginary part of Impedance*

Fig (e) shows the imaginary part of impedance (Z'') of the ferrites as a function of the natural logarithm of frequency ($\ln f$). The graph shows the impedance behavior of ZnFe_2O_4 which decreases with increasing frequency.

The graph also shows that $\text{Zn}_{0.5}\text{Ni}_{0.5}\text{Fe}_2\text{O}_4$, and $\text{Zn}_{0.5}\text{Co}_{0.5}\text{Fe}_2\text{O}_4$ has a different impedance behavior, which is almost constant with increasing frequency. This means that it has almost constant resistance and reactance [40].

5.5.5 *AC Conductivity*

Fig (f) shows the AC conductivity of the ferrites as a function of the natural logarithm of frequency ($\ln f$). AC conductivity is a measure of how well a material can conduct alternating current. It is related to the mobility and concentration of charge carriers in the material [42].

The graph shows that $\text{Zn}_{0.5}\text{Ni}_{0.5}\text{Fe}_2\text{O}_4$ and $\text{Zn}_{0.5}\text{Co}_{0.5}\text{Fe}_2\text{O}_4$ have similar AC conductivity behaviors, which increase linearly with $\ln f$. The AC conductivity depends on the hopping frequency and the concentration of charge carriers.

The dielectric studies of Zinc Ferrite, Zinc Cobalt Ferrite, and Zinc Nickel Ferrite reveal their frequency-dependent electrical behaviors arising from distinct underlying mechanisms. The dielectric constant decreases with increasing frequency, reflecting reduced responsiveness to electric fields. Zinc Ferrite and Zinc Nickel Ferrite exhibit dominant electron hopping, causing polarization and energy dissipation, while Zinc Cobalt Ferrite's behavior suggests Maxwell-Wagner relaxation at interfaces. These findings hold significance for supercapacitor electrode applications, as the materials' frequency-dependent dielectric properties align with efficient energy storage/release. Zinc Ferrite and Zinc Nickel Ferrite's electron hopping mechanism can enhance performance across

frequencies, while Zinc Cobalt Ferrite's behavior offers potential for specialized frequency-dependent applications, informing electrode design for diverse energy storage requirements [42].

5.6 Electrochemical Testing

The electrochemical tests, i.e., GCD and CV were performed by immersing the electrodes into a 2 M KOH solution as an electrolyte. In the investigation of an electrode for supercapacitor applications, one of the most important parameters is the electrode behavior during various scan rates.

The current density is a measure of how much electric charge flows through a unit area of the material. A higher current density means a higher rate of charge and discharge, which is the speed at which the battery can be filled or emptied. The potential is a measure of how much electric energy is stored in the material. A higher potential means a higher energy density, which is the amount of energy that can be stored per unit mass of the material.

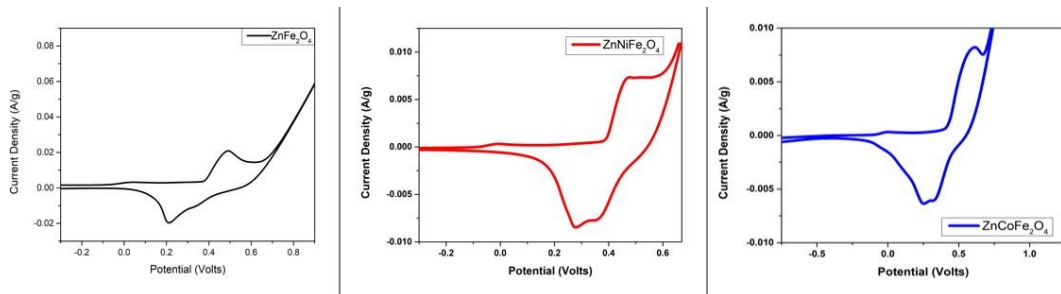


Figure 5.7: Cyclic Voltammetry properties of ZnFe_2O_4 , $\text{Zn}_{0.5}\text{Ni}_{0.5}\text{Fe}_2\text{O}_4$ and $\text{Zn}_{0.5}\text{Co}_{0.5}\text{Fe}_2\text{O}_4$ Nanoparticles

Zinc ferrite (ZnFe_2O_4) exhibits low redox activity and is considered electrochemically inert due to the mixed valence states of its iron (Fe) ions, which hinder reversible redox processes. Consequently, in cyclic voltammetry, ZnFe_2O_4 shows a relatively flat current response with minimal redox peaks, indicating limited electrochemical activity and rendering it less suitable for charge storage applications.[31] The graph (a) shows that ZnFe_2O_4 has a high-power density and a moderate energy density.

This means that it can deliver a lot of power in a short time, but it cannot store as much energy as some other materials. The graph has a minimum at around 0.2 volts and 0.02 A/g and a maximum at around 0.6 volts and 0.08 A/g. These points indicate the optimal operating range of ZnFe_2O_4 , where it can achieve the best performance in terms of power and energy density. The graph has a slight dip at around 0.4 volts and 0.04 A/g. This could be due to a phase transition or a structural change in the material, which affects its electrical properties.

On the other hand, zinc cobalt ferrite ($\text{Zn}_{0.5}\text{Co}_{0.5}\text{Fe}_2\text{O}_4$) displays more pronounced redox activity owing to the presence of cobalt (Co) ions, which readily undergo reversible redox reactions. This results in well-defined redox peaks in cyclic voltammetry, signifying higher electrochemical activity and suggesting potential applications in electrochemical energy storage devices.[32]

The graph (b) shows that $\text{Zn}_{0.5}\text{Co}_{0.5}\text{Fe}_2\text{O}_4$ has a low rate of charge and discharge and a low voltage. This means that it cannot deliver or store much energy compared to some other materials. The graph also shows that $\text{Zn}_{0.5}\text{Co}_{0.5}\text{Fe}_2\text{O}_4$ has a sharp peak at around -0.5 volts and 0.008 A/g and a sharp trough at around 0.0 volts and -0.004 A/g. This could be due to a redox reaction or a charge transfer in the material, which affects its electrical properties. The graph then flattens out and rises slightly to around 0.012 A/g at 0.5 volts. This could be due to saturation or a limitation of the material, which prevents it from increasing its current density or voltage further.

Similarly, zinc nickel ferrite (ZnNi_2O_4) shows noticeable redox behavior due to the presence of nickel (Ni) ions, and in cyclic voltammetry, distinct redox peaks corresponding to the reversible redox reactions of nickel ions can be observed. [33] The graph (c) shows that $\text{Zn}_{0.5}\text{Ni}_{0.5}\text{Fe}_2\text{O}_4$ has a low rate of charge and discharge and a low voltage. This means that it cannot deliver or store much energy compared to some other materials. The graph also shows that $\text{Zn}_{0.5}\text{Ni}_{0.5}\text{Fe}_2\text{O}_4$ has a sharp dip at around 0.2 volts and then rises sharply to around 0.005 A/g at 0.4 volts. This could be due to a redox reaction or a charge transfer in the material, which affects its electrical properties. The graph then flattens out and rises

slightly to around 0.010 A/g at 0.6 volts. This could be due to saturation or a limitation of the material, which prevents it from increasing its current density or voltage further.

This demonstrates ZnNiFe₂O₄'s favorable electrochemical characteristics, making it a promising candidate for applications in energy storage and electrocatalysis. Overall, the electrochemical behavior of these ferrite materials is influenced by the nature of their metal ions, with zinc cobalt ferrite and zinc nickel ferrite outperforming zinc ferrite in terms of redox activity and potential for electrochemical applications.

CHAPTER 6: CONCLUSIONS AND FUTURE RECOMMENDATION

6.1 Conclusion

In conclusion, this comprehensive study has provided valuable insights into the synthesis, characterization, and electrochemical behavior of Zinc Ferrite (ZnFe_2O_4), Zinc Cobalt Ferrite ($\text{Zn}_{0.5}\text{Co}_{0.5}\text{Fe}_2\text{O}_4$), and Zinc Nickel Ferrite ($\text{Zn}_{0.5}\text{Ni}_{0.5}\text{Fe}_2\text{O}_4$) nanoparticles, shedding light on their potential as supercapacitor electrodes. The investigation commenced with the successful co-precipitation synthesis of these ferrite materials, followed by meticulous purification and characterization using various analytical techniques.

X-ray Diffraction (XRD) analysis confirmed the formation of high-purity spinel structures for all three ferrites, with lattice parameters and crystallite sizes determined. These parameters contribute to their structural stability and potential for efficient charge storage. Scanning Electron Microscopy (SEM) revealed the nanometer-scale, spherical morphology of the nanoparticles, highlighting their suitability for supercapacitor applications. Energy-Dispersive X-ray Spectroscopy (EDS) confirmed the presence of zinc, iron, nickel, and cobalt, corroborating the successful incorporation of transition metal ions into the spinel lattice.

Raman spectroscopy further elucidated the distinctive vibrational characteristics of these ferrites, offering a discriminating means of differentiation. The peak intensities and positions provided insights into the unique behavior of these materials, with implications for their electrochemical performance.

Fourier Transform Infrared Spectroscopy (FTIR) unveiled distinct vibrational modes and bond strengths within the ferrite structures, with variations attributed to the presence of different metal ions. These findings underscore the potential for tailoring the electrochemical properties of these materials based on their compositions.

Dielectric studies provided valuable information on the frequency-dependent electrical behaviors of the ferrites, indicating their suitability for energy storage

applications. The electron hopping mechanism in Zinc Ferrite and Zinc Nickel Ferrite, along with Maxwell-Wagner relaxation in Zinc Cobalt Ferrite, offered a comprehensive understanding of their dielectric characteristics.

Electrochemical testing through Cyclic Voltammetry (CV) demonstrated the electrochemical activity of these materials, with Zinc Cobalt Ferrite and Zinc Nickel Ferrite displaying well-defined redox peaks, indicative of their potential as supercapacitor electrodes. The differential electrochemical behavior was attributed to the nature of the metal ions present in the ferrite structures.

In summary, this study has laid the foundation for the potential application of ZnFe_2O_4 , $\text{Zn}_{0.5}\text{Ni}_{0.5}\text{Fe}_2\text{O}_4$, and $\text{Zn}_{0.5}\text{Co}_{0.5}\text{Fe}_2\text{O}_4$ nanoparticles as promising supercapacitor electrodes. The combination of their unique structural, vibrational, and electrochemical properties positions them as candidates for advanced energy storage solutions.

6.2 Future Recommendations

The insights gained from this research contribute to the expanding knowledge base on advanced electrode materials for energy storage applications, paving the way for further optimization and exploration of these distinctive ferrite-based nanoparticulate systems. Future research can build upon these findings to develop high-performance supercapacitor devices and advance the field of energy storage.

REFERENCES

- [1] S. A. Ahire, A. A. Bachhav, T. B. Pawar, B. S. Jagdale, A. V. Patil, and P. B. J. R. i. C. Koli, "The augmentation of nanotechnology era: A concise review on fundamental concepts of nanotechnology and applications in material science and technology," p. 100633, 2022.
- [2] W. Chaikittisilp, Y. Yamauchi, and K. J. A. M. Ariga, "Material evolution with nanotechnology, nanoarchitectonics, and materials informatics: what will be the next paradigm shift in nanoporous materials?," vol. 34, no. 7, p. 2107212, 2022.
- [3] S. Kour, R. Jasrotia, N. Kumari, V. P. Singh, P. Singh, and R. Kumar, "A current review on synthesis and magnetic properties of pure and doped manganese ferrites," in *AIP Conference Proceedings*, 2022, vol. 2357, no. 1: AIP Publishing.
- [4] G. Datt, "Spinel ferrite-based heterostructures for spintronics applications," in *Ferrite Nanostructured Magnetic Materials*: Elsevier, 2023, pp. 747-773.
- [5] M. Umair, A. Quader, M. Imran, M. A. Yaqub, S. M. Ramay, and S. J. C. I. Atiq, "Significant impact of spinel ferrites in evolution of magneto-electric coupling in novel tri-phase composites," vol. 48, no. 10, pp. 14473-14480, 2022.
- [6] A. I. Borhan, D. Ghercă, A. R. Iordan, and M. N. J. F. N. M. M. Palamaru, "Classification and types of ferrites," pp. 17-34, 2023.
- [7] M. Arshad, M. A. Khan, G. A. Ashraf, K. Mahmood, and M. I. J. C. I. Arshad, "Investigation of crystal structure, electrical and dielectric response of Zr^{4+} - Co^{2+} substituted Ba-Sr-Ni Y-type hexagonal ferrites synthesized by sol-gel route," vol. 49, no. 3, pp. 4141-4152, 2023.
- [8] M. Wajad *et al.*, "Structural elucidation, morphological properties, and dielectric properties of nickel-substituted cobalt and lead-based X-type hexagonal ferrites," pp. 1-11, 2022.

- [9] S. I. J. J. o. M. Ahmad and M. Materials, "Nano cobalt ferrites: Doping, Structural, Low-temperature, and room temperature magnetic and dielectric properties—A comprehensive review," p. 169840, 2022.
- [10] Y. Mu, Z.-H. Ma, H.-S. Liang, L.-M. Zhang, and H.-J. J. R. M. Wu, "Ferrite-based composites and morphology-controlled absorbers," vol. 41, no. 9, pp. 2943-2970, 2022.
- [11] H. S. Jarusheh, A. Yusuf, F. Banat, M. A. Haija, and G. J. J. o. E. C. E. Palmisano, "Integrated photocatalytic technologies in water treatment using ferrites nanoparticles," p. 108204, 2022.
- [12] S. R. Mokhosi, W. Mdlalose, A. Nhlapo, and M. J. P. Singh, "Advances in the synthesis and application of magnetic ferrite nanoparticles for cancer therapy," vol. 14, no. 5, p. 937, 2022.
- [13] S. Sayah *et al.*, "How do super concentrated electrolytes push the Li-ion batteries and supercapacitors beyond their thermodynamic and electrochemical limits?," vol. 98, p. 107336, 2022.
- [14] A. Dutta, S. Mitra, M. Basak, and T. J. E. S. Banerjee, "A comprehensive review on batteries and supercapacitors: development and challenges since their inception," vol. 5, no. 1, p. e339, 2023.
- [15] G. Jiang, R. A. Senthil, Y. Sun, T. R. Kumar, and J. J. J. o. P. S. Pan, "Recent progress on porous carbon and its derivatives from plants as advanced electrode materials for supercapacitors," vol. 520, p. 230886, 2022.
- [16] M. S. Javed *et al.*, "The quest for negative electrode materials for Supercapacitors: 2D materials as a promising family," vol. 452, p. 139455, 2023.
- [17] A. Manohar, V. Vijayakanth, S. P. Vattikuti, and K. H. J. C. I. Kim, "Structural and electrochemical properties of mixed calcium-zinc spinel ferrites nanoparticles," vol. 49, no. 3, pp. 4365-4371, 2023.

- [18] A. K. Ghasemi, M. Ghorbani, M. S. Lashkenari, and N. J. J. o. E. S. Nasiri, "Controllable synthesis of zinc ferrite nanostructure with tunable morphology on polyaniline nanocomposite for supercapacitor application," vol. 51, p. 104579, 2022.
- [19] J. M. Gonçalves *et al.*, "Sensing performances of spinel ferrites MFe_2O_4 (M= Mg, Ni, Co, Mn, Cu and Zn) based electrochemical sensors: A review," vol. 1233, p. 340362, 2022.
- [20] D. Parajuli, V. Vagolu, K. Chandramoli, N. Murali, and K. J. J. o. N. P. S. Samatha, "Electrical Properties of Cobalt Substituted NZCF and ZNCF Nanoparticles Prepared by the Soft Synthesis Method," vol. 8, no. 3, pp. 45-52, 2022.
- [21] B. Babukutty, D. Ponnamma, S. S. Nair, and S. J. R. i. M. Thomas, "Correlating the rheological and magneto-optical properties of cobalt substituted magnetite ferrofluids ($Co_xFe_{1-x}Fe_2O_4$) with theoretical studies," vol. 17, p. 100382, 2023.
- [22] T. A. Wani, G. Suresh, R. Masrour, K. M. Batoo, A. J. M. C. Rasool, and Physics, "A structural, morphological, optical and magnetic study of nickel-substituted zinc (Ni-Zn) ferrite nanoparticles synthesized via glycine assisted gel autocombustion synthesis route," vol. 307, p. 128169, 2023.
- [23] D. Chahar, P. Thakur, A.-C. A. Sun, and A. J. J. o. M. S. M. i. E. Thakur, "Investigation of structural, electrical and magnetic properties of nickel substituted Co-Zn nanoferrites," vol. 34, no. 10, p. 901, 2023.
- [24] M. Ates, O. Kuzgun, and I. J. I. P. J. Candan, "Supercapacitor performances of titanium-polymeric nanocomposites: a review study," pp. 1-27, 2022.
- [25] L. Yan *et al.*, "Regulating the specific surface area and porous structure of carbon for high performance supercapacitors," vol. 615, p. 156267, 2023.
- [26] T. Sun *et al.*, "Boosting supercapacitor performance through the facile synthesis of boron and nitrogen co-doped resin-derived carbon electrode material," vol. 138, p. 110258, 2023.

- [27] P. R. Kharangarh, N. M. Ravindra, G. Singh, and S. J. J. o. E. S. Umapathy, "Synthesis and characterization of Nb-doped strontium cobaltite@ GQD electrodes for high performance supercapacitors," vol. 55, p. 105388, 2022.
- [28] S.-H. Kim *et al.*, "Atom probe analysis of electrode materials for Li-ion batteries: challenges and ways forward," vol. 10, no. 9, pp. 4926-4935, 2022.
- [29] A. R. Xavier, A. Ravichandran, S. Vijayakumar, M. D. Angelin, S. Rajkumar, and J. P. J. J. o. M. S. M. i. E. Merlin, "Synthesis and characterization of Sr-doped CdO nanoplatelets for supercapacitor applications," vol. 33, no. 11, pp. 8426-8434, 2022.
- [30] O. Folorunso, P. O. Olukanmi, and T. J. E. R. Shongwe, "Progress towards sustainable energy storage: A concise review," p. e12731, 2023.
- [31] S. Sahoo, R. Kumar, E. Joanni, R. K. Singh, and J.-J. J. J. o. M. C. A. Shim, "Advances in pseudocapacitive and battery-like electrode materials for high performance supercapacitors," vol. 10, no. 25, pp. 13190-13240, 2022.
- [32] M. Lewandowski, M. Bartoszewicz, K. Jaroszevska, G. J. J. o. I. Djéga-Mariadassou, and E. Chemistry, "Transition metal borides of Ni-B (Co-B) as alternative non-precious catalytic materials: Advances, potentials, and challenges. Short review," 2022.
- [33] N. Abid *et al.*, "Synthesis of nanomaterials using various top-down and bottom-up approaches, influencing factors, advantages, and disadvantages: A review," vol. 300, p. 102597, 2022.
- [34] L. Krishnia, P. Thakur, and A. Thakur, "Synthesis of nanoparticles by physical route," in *Synthesis and Applications of Nanoparticles*: Springer, 2022, pp. 45-59.
- [35] K. R. J. N. Jagdeo and F. CRC Press: Boca Raton, USA, "Physical Methods for Synthesis of Nanoparticles," pp. 66-76, 2023.
- [36] J. Maroušek *et al.*, "Silica nanoparticles from coir pith synthesized by acidic sol-gel method improve germination economics," vol. 14, no. 2, p. 266, 2022.

- [37] A. Salabat and F. J. P. C. Mirhoseini, "Polymer-based nanocomposites fabricated by microemulsion method," vol. 43, no. 3, pp. 1282-1294, 2022.
- [38] I. Shahzadi *et al.*, "Hydrothermal Synthesis of Fe-Doped Cadmium Oxide Showed Bactericidal Behavior and Highly Efficient Visible Light Photocatalysis," vol. 8, no. 33, pp. 30681-30693, 2023.
- [39] K. Hachem *et al.*, "Methods of chemical synthesis in the synthesis of nanomaterial and nanoparticles by the chemical deposition method: A review," vol. 12, no. 3, pp. 1032-1057, 2022.
- [40] A. Ali, Y. W. Chiang, and R. M. J. M. Santos, "X-ray diffraction techniques for mineral characterization: A review for engineers of the fundamentals, applications, and research directions," vol. 12, no. 2, p. 205, 2022.
- [41] S. Srujana and D. J. N. f. E. E. Bhagat, "Chemical-based synthesis of ZnO nanoparticles and their applications in agriculture," vol. 7, no. 1, pp. 269-275, 2022.
- [42] Y. Tkachenko and P. J. M. Niedzielski, "FTIR as a method for qualitative assessment of solid samples in geochemical research: A review," vol. 27, no. 24, p. 8846, 2022.
- [43] A. Ntziouni *et al.*, "Review of Existing Standards, Guides, and Practices for Raman Spectroscopy," vol. 76, no. 7, pp. 747-772, 2022.
- [44] X. Zhang, Z. Yugang, and Y. J. C. J. o. A. Chun, "Recent developments in thermal characteristics of surface dielectric barrier discharge plasma actuators driven by sinusoidal high-voltage power," vol. 36, no. 1, pp. 1-21, 2023.
- [45] R. A. Wong, Y. Yokota, and Y. J. C. O. i. E. Kim, "Stepping beyond cyclic voltammetry: Obtaining the electronic and structural properties of electrified solid – liquid interfaces," vol. 34, p. 100964, 2022.
- [46] M. Mallapur *et al.*, "Structural and electrical properties of nanocrystalline cobalt substituted nickel zinc ferrite," vol. 479, no. 1-2, pp. 797-802, 2009.

